

NEW FLAVOR PRODUCTION IN  $\gamma$ ,  $\mu$ ,  $\nu$ , AND HADRON BEAMS\*

Stanley Wojcicki  
 Physics Department and  
 Stanford Linear Accelerator Center  
 Stanford University, Stanford, California 94305

INTRODUCTION

During the last few years, the main emphasis in the study of heavy particle production (i.e. mainly charm) by other means than  $e^+e^-$  annihilation has been on the production mechanisms. Because of the relative cleanliness of the charm signal in the  $e^+e^-$  process, most of the data on the properties of the charm particles has originated from that source. There are already indications, however, that this situation is changing. Improved detection techniques coupled with much higher intrinsic production rates suggest that in the future the study of the properties of charm particles will cease to be an exclusive domain of  $e^+e^-$  machines.

This review, however, will concentrate mainly on the production data in the  $\gamma$ ,  $\mu$ ,  $\nu$  and hadron beams. This is partly because the decay properties have been covered in the review talk of George Trilling and partly because up to now most experiments did emphasize mainly the production aspects. In addition there has been recently a considerable interest in trying to explain most of these data phenomenologically by use of first order QCD diagrams, i.e. photon

gluon fusion diagram (Fig. 1a) in the case of photo and muon-production of charmed hadrons and gluon-gluon or quark-quark fusion (Fig. 1b,c) and charmed sea excitation (Fig. 1d,e) for hadronic production of charmed particles. These mechanisms relate the quark structure functions as measured in the massive di-lepton pair production experiments and the deep inelastic scattering experiments ( $\mu$ ,  $e$ , and  $\nu$ ) to the production distribution of the charmed hadrons. In addition the gluon diagrams, if dominant, allow one to measure the gluon distributions of the  $\pi$ ,  $K$ , and the nucleon.

One can contrast this situation with the production of charmed particles in the neutrino interactions either via interaction of the W boson with a strange

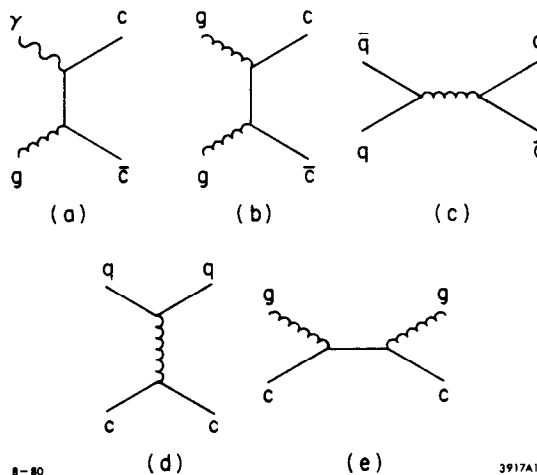
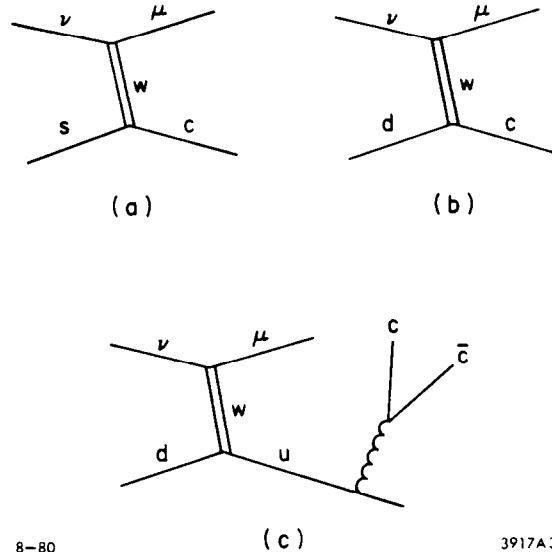


Fig. 1. Typical 1st order QCD diagrams for open charm production by photons and hadrons: a)  $\gamma g \rightarrow c\bar{c}$ , b)  $gg \rightarrow c\bar{c}$ , c)  $q\bar{q} \rightarrow c\bar{c}$ , d)  $qc \rightarrow qc$ , e)  $gc \rightarrow gc$ .

\*Work supported by the Department of Energy, contract DE-AC03-76SF00515, and the National Science Foundation.

(Invited talk presented at the XXth International Conference on High Energy Physics, University of Wisconsin, Madison, July 17-23, 1980.)

quark from the sea (Fig. 2a), or alternatively via Cabibbo suppressed  $d \rightarrow c$  quark transition (for antineutrinos only) (Fig. 2b). The interest here is mainly the  $x$  distribution of the strange sea, which can be extracted from the di-lepton production in the neutrino interactions. That subject (i.e.  $\mu^+\mu^-$  and  $\mu^\pm e^\mp$  production) has been covered adequately in Frank Sciulli's talk and will not be discussed further here. On the other hand QCD diagrams similar to the ones discussed above (e.g. Fig. 2c) are relevant to the question of associated production of the charmed particles in neutrino interactions, and the data relevant to that question will be summarized briefly.



8-80

3917A36

Fig. 2. Diagrams for charm production by neutrinos: a) off strange quark sea, b) off down quark, c) associated production.

#### EXPERIMENTAL COMMENTS

The heavy flavor searches divide themselves naturally into 3 different categories, each one characterized by its own peculiar advantages and shortcomings. We shall summarize them here very briefly:

(1) Peaks in the invariant mass spectra. This is the classical method of searching for very short lived particles and has been extremely successful in unraveling the old spectroscopy. It becomes more difficult as masses and beam energies increase, mainly because of rapidly growing number of combinatorials. Furthermore, these kinds of experiments, if performed with electronic techniques, generally investigate only a very limited region of phase space, so extraction of total cross section or angular distribution becomes very model dependent. Finally another potential danger with this technique, especially important when the statistics are limited, is the difficulty of interpreting correctly the statistical significance of a peak in the presence of a large number of cuts. The cuts will be naturally chosen so as to maximize the peaks and thus raise the danger of overemphasizing statistical fluctuations. On the other hand, the mass peak method provides the cleanest way to identify production of specific states (e.g.  $\Lambda_c$ ,  $F^+$ ,  $D^0$ , etc.).

(2) Semileptonic decay modes (i.e. detection of prompt  $\nu$ ,  $e$ , or  $\mu$  and of muon polarization). Here most of the information on the parent particle is lost so identification of specific states is impossible. In addition, because of widely varying semileptonic branching ratios for different charm particles (see below) extraction of total cross section becomes difficult unless contribution of specific

states is known from other sources. Furthermore, the initial production features are somewhat degraded since one observes second generation particles. On the other hand, the important plus here is the possibility of obtaining rather good statistics with a good signal to noise ratio.

(3) Search for short tracks (emulsions, high resolution streamer chambers and bubble chambers, solid state detectors). Most of these detectors are at present undergoing vigorous development efforts and they will probably play a much more important role in the future. Except for the neutrino emulsion experiments, most of these techniques have so far only demonstrated feasibility of doing heavy flavor experiments but as yet their impact on the field has not been very great. Their obvious advantages are relatively bias-free identification of heavy particles, possibility to study in detail the systematics of these particles, and simultaneous exploration of the full  $4\pi$  solid angle. One important shortcoming so far has been the relatively low event rate and a great deal of scanning effort necessary to extract the interesting events.

In practice, of course, these techniques are not orthogonal, and very frequently a given experiment will simultaneously rely on use of more than just one of these techniques.

Several additional experimental comments may be in order here.

(a) The relative ratio of charm to non charm hadron production is strongly dependent on the nature of the beam. The rough orders of magnitude for different beams are;

$$\begin{array}{ll}
 \text{hadronic beams} & \sim 10^{-3} \\
 \text{photon } (\mu) \text{ beams} & \sim 10^{-2} \\
 \text{neutrino beams} & \sim 10^{-1} \\
 e^+e^- \text{ annihilation} & \sim 1
 \end{array}$$

(b) The evidence presented at this conference provides strong evidence that the lifetimes of different charm particles differ widely. The most systematic study of this question was presented in a report by Niu, who quoted<sup>1)</sup>

$$\left. \begin{array}{l}
 D^+ \rightarrow 10.3 \begin{array}{l} +10.5 \\ -4.1 \end{array} \\
 D^0 \rightarrow 1.01 \begin{array}{l} +.43 \\ -.27 \end{array} \\
 F^+ \rightarrow 2.2 \begin{array}{l} +2.8 \\ -1.0 \end{array} \\
 \Lambda_c \rightarrow 1.36 \begin{array}{l} +0.84 \\ -0.46 \end{array}
 \end{array} \right\} \times 10^{-13} \text{ sec}$$

The significance of this result in the content of the present discussion is that the semileptonic branching ratios will be approximately proportional to the lifetime (that statement is rigorously true for  $D^+$  and  $D^0$ ). Thus all the cross section estimates extracted from the semileptonic experiments might be significantly in error if the production process is dominated by one single state.

(c) A dependence of the cross section is a relevant question here. Since most fixed target experiments use generally heavy nuclei as target material (e.g. iron,  $A = 56$ ) and ISR experiments study p-p interactions, knowledge of A dependence is quite crucial to the comparison of different experiments. It is conventional now to assume linear A dependence for heavy flavors, in analogy with the  $J/\psi$  production<sup>2)</sup>. However, it should be stressed here that at present there are no experiments that bear on this question for unbound charm production, and that the A dependence could vary with x.

#### CHARM PRODUCTION BY HADRONS

The field of hadronic production of unbound charm states (i.e.  $D$ ,  $\Lambda_c$ , etc.) is still in its early infancy. Because of rather unfavorable signal to noise ratio only very sparse data on production rates are available and the information on x and  $p_T$  distributions is even more scanty. Thus only very rough comparisons with phenomenological predictions can be made; this section, accordingly, shall emphasize mainly the experimental data and the outstanding experimental problems. More specifically, we shall address 3 separate topics here, i.e.

- 1) Central Production, Near  $x = 0$
- 2) The Question of Forward Production
- 3) Anomalies and Disagreements Between Different Experiments.

1) Central Production. I shall try to summarize here the contributions of all those experiments that either concentrated on  $x = 0$  region or had such acceptance that they were sensitive to the production in that region. No firm quantitative predictions and comparisons with the theory can be made here with any strong degree of assurance. This is at least partly due to potential contribution of several different diagrams (quark fusion, gluon fusion, flavor excitation by quark or gluon scattering), our ignorance about their relative importance,<sup>3)</sup> and dependence of the calculations on the mass of the charmed quark. On the other hand we can make some reasonably intelligent guesses as to what the hadronic production of charm should look like if the diagrams discussed above were indeed the dominant ones. Specifically we would expect:

- a) The cross section in the Fermilab and SPS region ( $\sqrt{s} \approx 30$ ) to be about 5-20  $\mu\text{b}$  for total charm production.
- b) The increase between that energy domain and the ISR energy range ( $\sqrt{s} \approx 60$ ) should be about a factor of 2-3.
- c) The x distribution for production by nucleons should go roughly as  $(1-x)^n$  with n being somewhere between 3 and 5, since that is the approximate dependence of the quark and gluon distributions in the nucleon. Mesonic production distribution might be expected to be slightly flatter.

The data available up to now are summarized in Table I. Several observations need and can be made regarding these data.

- a) The comparison between different numbers should probably not be taken more seriously than up to a factor of 2. This is because of unknowns in A dependence, branching ratios, final states produced, and

TABLE I

Summary of charm cross section results

Reaction	Group	Reference	Technique	Signature	$\sqrt{s}$	$\sigma(\mu\text{b})$
$\pi^- p$	BGRST	4	TST in BEBC	Single e	11.5	$19 \pm 11$
$\pi^- \text{Be}$	PSTB	5	$D^*$ only	$(K\pi)\pi$	19.4	$10 \pm 4$
$\bar{p}p$	BHLMS	6	TST in BEBC	Single e	11.5	$< 24$
$\pi^- p$	BCOPRRT	7	LEBC	Short tracks	25.6	35-40
$p\text{Em}$	Tata	8	emulsion	Short tracks	27.4	$160 \pm 40$
$pp$	CERN-Saclay -Zurich	9	spectrometer	$\mu^\pm e^\mp, e^\pm e^\mp$	53, 63	$22 \pm 5$
$p\text{Ne}$	Yale-Fermilab	10	streamer ch.	Short tracks	25.8	20-50
$p\text{Em}$	Nagoya-Aichi- Yokohama	11	emulsion	Short tracks	27.4	$30 \pm 20$
$p\text{Fe}$	CIT-Stanford	12	total absorption	Single $\mu$	27.4	13-60
$p\text{Fe}$	CIT-Stanford	13	total absorption	$2\mu + \text{ME}$	27.4	7-20
$p\text{Fe}$	CFRS	14	total absorption	Single $\mu$	25.8	$22 \pm 9$
$p\text{Fe}$	Serpukhov	15	beam dump	$\nu$	11.5	$4 \pm 3$
$p\text{W}$	Michigan	16	beam dump (test)	$\nu$	27.4	30-75
$p\text{Cu}$	Gargamelle	17	beam dump	$\nu$	27.4	$80^{+40}_{-25}$
$p\text{Cu}$	BEBC	18	beam dump	$\nu$	27.4	11-22
$p\text{Cu}$	CDHS	18	beam dump	$\nu$	27.4	7-14
$p\text{Cu}$	CHARM	19	beam dump	$\nu$	27.4	$12 \pm 4$
$pp$	ACCDHW	20	SFM, $e^-$ trigger	$\Lambda_c^- \rightarrow K^- \pi^+ p$	63	$140 \pm 60^*$
$pp$	ACCDHW	20	SFM, $e^-$ trigger	$D^0 \rightarrow K^- \pi^+$	63	$700 \pm 300^*$

\*  $\frac{d\sigma}{dx_F}$  at  $x_F = 0$

8-80  
3917A37

production mechanisms. No great effort has been made to insure that the assumptions used in extracting the final numbers for all the experiments have been entirely self consistent.

b) The data are dominated by the experiments near  $\sqrt{s} \approx 27$ . In that region, the total cross sections are consistent (up to a factor of 2) with  $\sigma_{\text{tot}} \approx 20 \mu\text{b}$ . The only point that appears to be slightly high is the preliminary result quoted by the Tata group<sup>8)</sup> at this conference of  $160 \pm 40 \mu\text{b}$ .

c) To the extent that the data on this question are available the experiments are consistent with central production, i.e. x dependence of the form  $(1-x)^n$  with  $3 < n < 5$ .

d) The situation in the ISR region near  $x = 0$  is not clear as there appears some discrepancy between the 3 different ISR measurements quoted. The question as to whether the cross section at  $x = 0$  rises dramatically between  $\sqrt{s} = 27$  and 60 does not appear to be settled by these data.

2) Forward Production. There have now been several experimental programs that bear on this question.

a) at  $\sqrt{s} = 53$  and 63 there are 3 experiments (by Split Field Magnet group,<sup>21)</sup> Lamp-Shadow Magnet group,<sup>22)</sup> and UCLA-Saclay group<sup>23)</sup>) that study  $\Lambda_c$  and D production at the ISR.

b) at  $\sqrt{s} = 27$  there are the 3 beam dump experiments (CDHS,<sup>24)</sup> BEBC,<sup>25)</sup> and CHARM<sup>19)</sup> collaborations) that study prompt  $\nu$  interactions (presumably coming from the decay of short-lived particles). In addition, the Cal Tech-Stanford collaboration has studied the production of prompt forward muons<sup>26)</sup> (presumably decay products of short-lived particles produced by the primary protons).

c) at  $\sqrt{s} = 20$ , a Fermilab experiment has studied forward diffractive production of D's in  $\pi^-p$  interactions.<sup>27)</sup>

d) at  $\sqrt{s} = 7.4$  there have been 3 beam dump experiments performed at the Brookhaven AGS.<sup>28)</sup>

Very briefly, the results of these experiments can be summarized as follows. Starting with the lowest energies, there appears to be no evidence for any prompt neutrino production in the BNL beam dump experiments. There is some discrepancy between the calculated  $\nu_\mu$  fluxes (coming from  $\pi$  and K decays from the original hadronic cascade) and the observed  $\nu_\mu$  numbers,<sup>29)</sup> but the majority belief is that the calculations probably are not reliable enough to make the discrepancy significant.<sup>30)</sup> The cross-section limits for charmed particle production as obtained from these experiments<sup>30)</sup> are still considerably above the interesting limits ( $12-20\mu\text{b}$  for  $\sigma_{\text{DD}}^- B_{\text{D} \rightarrow \nu_e}$ ).

For completeness one should mention here an older beam dump experiment performed at Serpukhov,<sup>15)</sup> i.e. intermediate energy ( $E_p = 70\text{GeV}$ ,  $\sqrt{s} = 11.5$ ). They report evidence for prompt  $\nu_e$  with a cross section,  $\sigma_{\text{DD}}^- B_{\text{D} \rightarrow \nu_e} = .5 \pm .4\mu\text{b}$ .

A finite signal for diffractive  $\text{D}\bar{\text{D}}$  production was obtained at Fermilab by the HFIOI collaboration<sup>27)</sup> in  $\pi^-p$  interactions at  $\sqrt{s} = 20$ . The evidence for production of roughly equal amounts of  $\text{D}^0$  and  $\bar{\text{D}}^0$  is displayed in Fig. 3b,c, where a narrow peak at the mass of the D is

seen in both the  $K^- \pi^+ \pi^+$  and the  $K^+ \pi^- \pi^-$  mass spectra. Furthermore, the  $x$  distribution (Fig. 3a) supports the hypothesis that the D's are produced diffractively, although it should be pointed out that the trigger itself requires a slow proton thus favoring a forward mechanism. A model dependent cross section estimate yields  $\sigma_{D\bar{D}} = (6-10) \pm 4 \mu\text{b}$ .

Turning now to  $\sqrt{s} = 27$ , there is an agreement (within a factor of 2) between the CERN beam dump experiments and the Stanford-Cal Tech experiment at Fermilab on the overall size of the prompt lepton signal (the discrepancies on the details will be discussed below). As an example, Fig. 4 compares the momentum distribution of the prompt lepton from the Fermilab and BEBC experiments. The techniques are totally different here; the comparison is relatively model independent. Some model dependence arises from the fact that the acceptance in the  $p_T$ - $x$  space is quite different for these 2 experiments. Both experiments are sensitive to a large fraction of the forward  $x$  region; however the Stanford-CIT experiment has basically a flat 100% acceptance for  $p_\mu > 60 \text{ GeV}$ ; the relative detection efficiency for the beam dump experiments goes roughly as  $p_\nu^3$ . Furthermore the Stanford-CIT experiment accepts essentially all  $p_T$ ; the neutrino experiments look only at very low  $p_T$  ( $\Delta\theta \leq 1.8 \text{ mrad}$ ).

The gross features of the CERN experiments can be adequately explained by a central production.

Fig. 4. Comparison of the prompt  $\mu$  spectrum (CIT-Stanford) with prompt  $\nu$  spectrum (BEBC).

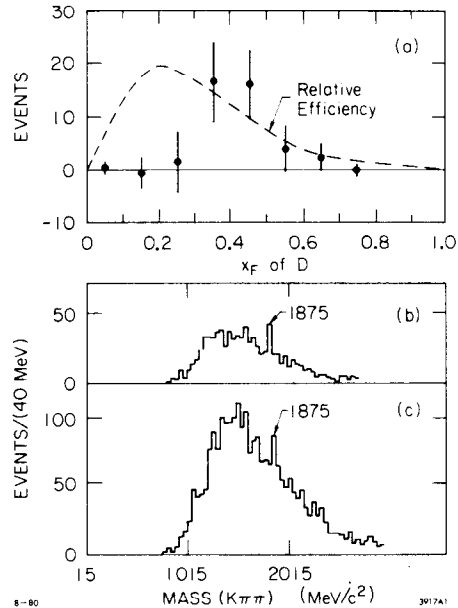
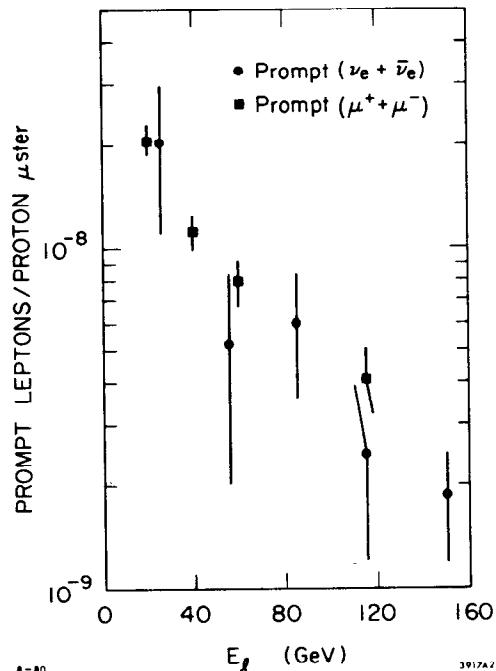


Fig. 3. a)  $x_F$  distribution of the events in the D peak, b)  $K^- \pi^+ \pi^+$  mass spectrum, c)  $K^+ \pi^- \pi^-$  mass spectrum.



mechanism that is consistent with that deduced by Stanford-CIT collaboration from their earlier experiments<sup>12,13)</sup> that emphasized the central region. In addition, a diffractive mechanism is not a good fit to the Stanford-CIT  $p_\mu$  distribution, predicting too many high energy muons. If the data are forced to a diffractive fit, the cross section estimate is  $14 \pm 4 \mu\text{b}$ .

Turning now to the ISR energies, we note the large forward production of charmed particles, especially  $\Lambda_c$ . The extraction of total production cross section is difficult and highly model dependent because in all experiments only a limited kinematic region is investigated. I shall try to summarize the relevant facts in as coherent a way as possible for both  $\Lambda_c$  and D production.

$\Lambda_c$  Production. The LSM and SFM groups have presented 2 measurements of  $\Lambda_c$  production.<sup>21,22)</sup> Both experiments identify the  $\Lambda_c \rightarrow K^- p \pi^+$  mode so they can be compared directly. Furthermore each experiment obtains one cross section measurement at a rather forward  $x$  by triggering on a  $K^-$ , and another one at a lower  $x$  by using an electron trigger (presumably from the accompanying  $\bar{\Lambda}_c$  or  $\bar{D}$ ). A universal 10% BR into electrons is assumed in extracting the cross section. Some of the representative plots from these experiments are displayed in Figs. 5 and 6 for the  $K^-$  trigger and Figs. 7 and 8 for the e trigger. There is some indication of a  $\bar{\Lambda}_c$  peak in the LSM data but the evidence is not totally conclusive because of low statistics and a slight downward displacement of the position of that mass peak.

One should also mention here an older published result by the UCLA-Saclay group<sup>23)</sup> who found a peak in the mass spectrum of both  $K^- p \pi^+$  and  $(\Lambda 3\pi)^+$  at very forward  $x$ . The results of all those  $K^- p \pi^+$  experiments are summarized in Fig. 9. There is still some model dependence inherent in those points because of finite  $\Delta x$  region explored and the requirement of an electron trigger for some of the data.

It is clear from Fig. 9 that the UCLA point does not appear compatible with other measurements unless some anomaly occurs near  $x=1$ . This would be very hard to understand simply on kinematical grounds as even most diffractive models would tend to give suppression of

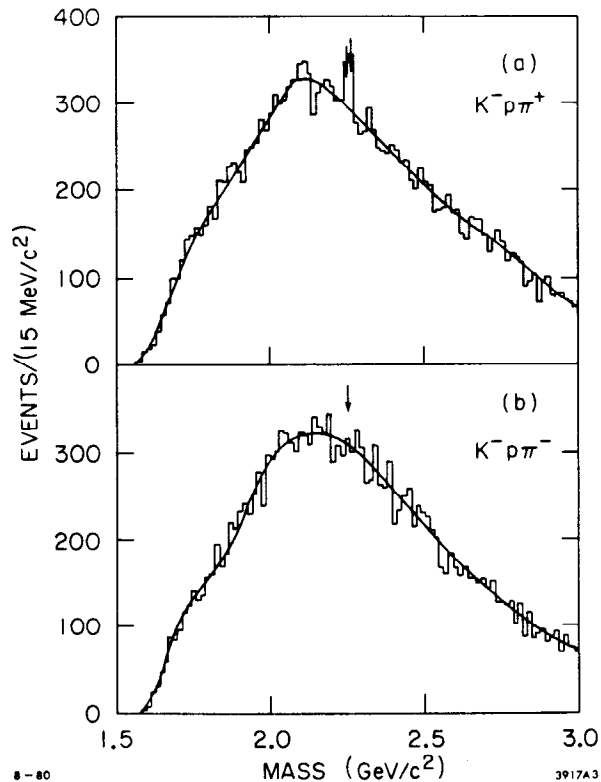


Fig. 5.  $K^- p \pi^+$  and b)  $K^- p \pi^-$  mass spectrum from the LSM experiment ( $K^-$  trigger).



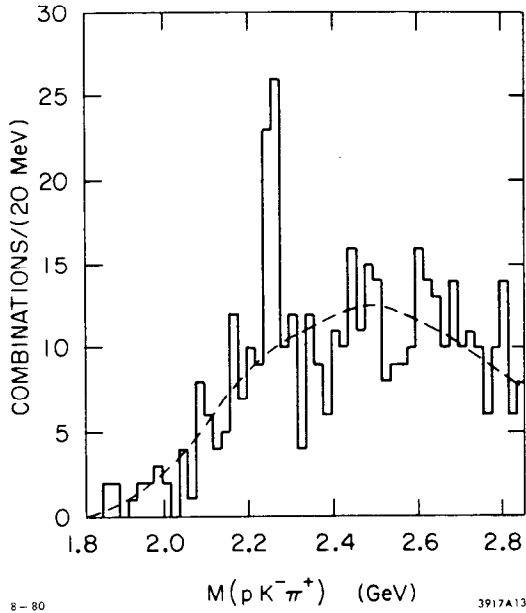


Fig. 6.  $K^- p \pi^+$  spectrum from the SFM experiment ( $K^-$  trigger).

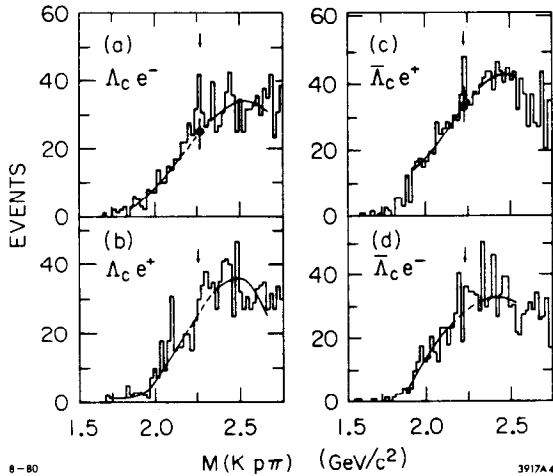


Fig. 7.  $K^- p \pi^+$  mass spectrum from the LSM experiment with the  $e^-$  (a) and  $e^+$  (b) trigger and the  $K^+ \bar{p} \pi^-$  spectrum with  $e^+$  (c) and  $e^-$  (d) triggers.

$\Lambda_c$  production in that region due to the large mass of  $\Lambda_c$  and accompanying  $\bar{D}$ . Ignoring the UCLA point we can extract a rough estimate of the total cross section by assuming a typical diffractive picture of flat  $x$  dependence up to  $x \approx 0.7$ .  $\sigma_{\text{tot}}$  will then be given by  $2 \cdot 0.7 \cdot B \frac{d\sigma}{dx} / B$ . Taking  $5 \mu\text{b}$  for  $B \frac{d\sigma}{dx}$  and  $2.2 \pm 1.0\%$  for  $K^- p \pi^+$  branching ratio<sup>31)</sup> we obtain  $320 \mu\text{b}$  for  $\sigma_T$ . This number should be compared with  $\sigma_T B(\Lambda_c^+ \rightarrow \Lambda 3\pi) = (1.0 \pm 0.3) \mu\text{b}$  extracted with the help of a diffractive production model by D. DiBitonto<sup>32)</sup> from a different subset of the LSM data. No good data exist allowing one to relate branching ratios for these two decay modes but it is unlikely that  $B(\Lambda_c \rightarrow 3\pi)$  is less than 1%. Thus we are faced with a discrepancy of at least a factor of 3.

We must remember that we have to add the D and F production to the above numbers to obtain total charm cross section. The indications from SFM are that the D cross section<sup>20)</sup> is also around several hundred  $\mu\text{b}$  implying a total charm cross section in the vicinity of  $1 \text{mb}$ , i.e.  $1\frac{1}{2}$  orders of magnitude above the cross sections observed at  $\sqrt{s} = 27$ . Is that reasonable and can it be easily understood? Let us examine some of the possible mechanisms for this difference:

1. Standard QCD diagrams would predict only a factor of 2 or so between  $\sqrt{s} = 30$  and  $60$ . A possibility is contribution from a different process (e.g. hidden intrinsic charm in the nucleon<sup>33)</sup>) with a sharp threshold near  $\sqrt{s} = 30$ . The assumption about a threshold appears slightly artificial.

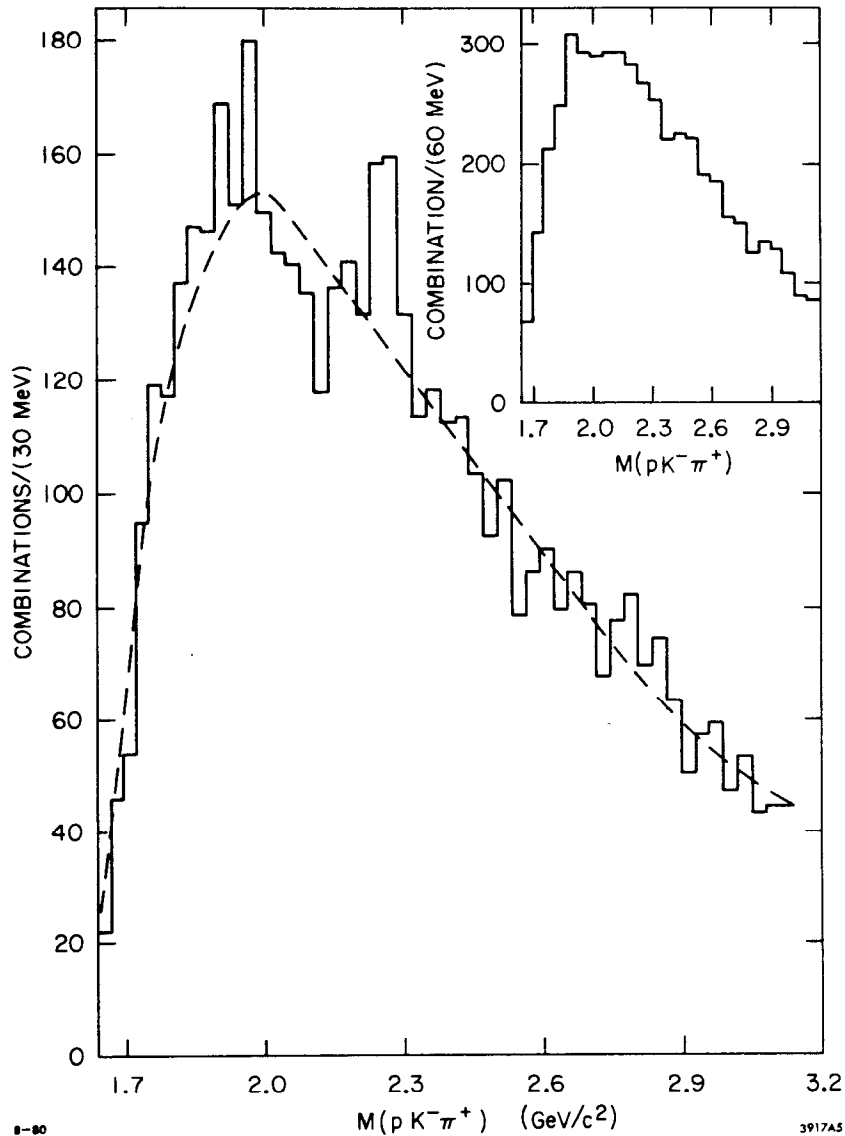


Fig. 8.  $K^- p \pi^+$  spectrum from the SFM experiment with the  $e^-$  trigger. Insert shows this spectrum with the  $e^+$  trigger.

2. A dependence could be closer to  $A^{0.75}$  for diffractive production.

3. Very low semileptonic branching ratio of  $\Lambda_c$  (there is certainly some evidence for that - see above<sup>1</sup>) would decrease the sensitivity of the beam dump and CIT-Stanford experiments.

4. The error on  $\Lambda_c \rightarrow K^- p \pi^+$  is still rather large. Thus a branching ratio larger by  $\sim 50\%$  certainly cannot be excluded.

Each of these effects could certainly contribute a factor of 2-3 making the cross section difference much more reasonable. One outside possibility that has to be considered is whether the effect that is seen at the ISR is really a  $\Lambda_c$  as opposed to a non-charmed resonant

state. It must be remembered that  $K^-p\pi^+$  is not an exotic state, and thus does not constitute a prima facie evidence for charm production. The association with charm is based on

- a) narrow width of the state
- b) absence of negative state
- c) mass comparable to  $\Lambda_c$  in  $e^+e^-$  annihilation
- d) association with electrons.

The first two pieces of evidence are really not very strong. Narrow non-charm states have been seen, and positive states are expected to dominate in pp collisions in the diffractive region. The latter is empirically observed for  $\Sigma(1385)$ .<sup>23)</sup> The mass question has been a source of controversy for some time and it might be worthwhile to consider the new contributions on this subject.

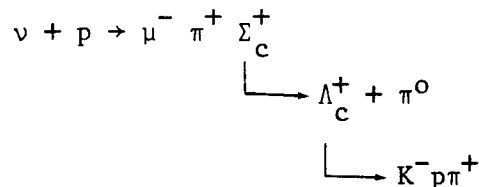
The masses of  $\Lambda_c$  have varied from 2255 to 2290 MeV but the recent data appear to favor a value of 2285 MeV. To summarize the recent measurements we have

$$M_{\Lambda_c} = 2.285 \pm 0.006 \text{ GeV} \quad e^+e^- \text{ SPEAR}^{31)}$$

$$M_{\Lambda_c} = 2.284 \pm 0.005 \text{ GeV} \quad \gamma p \text{ (CIF)}^{34)}$$

In addition there have been 3 contributions to this conference from the neutrino experiments that favor this value, i.e.

- a) a mass peak observed at  $2.275 \pm 0.010$  in  $\nu D$  interactions in  $\Lambda\pi^+$  and  $K_S^0 p$  (see Fig. 10)<sup>35)</sup>
- b) 2 completely fitted events from BEBC<sup>36)</sup> giving  $K^-p\pi^+$  masses of  $2.285 \pm 0.005$  and  $2.280 \pm 0.003$  GeV.
- c) a fully reconstructed BEBC TST event<sup>37)</sup>



giving  $M_{\Lambda_c} = 2290 \pm 0.003$ .

In contrast both LSM and SFM give consistently values around

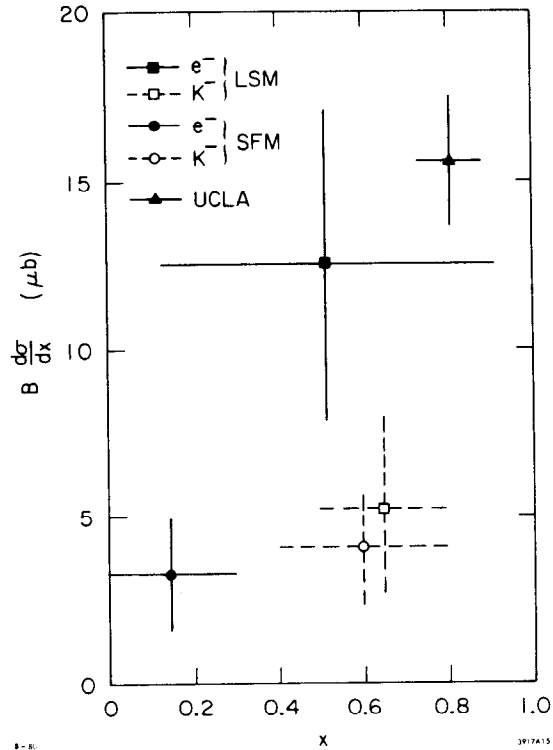


Fig. 9. Summary of the ISR  $K^-p\pi^+$  data.

2.260 GeV. It is hard to visualize a mechanism that would give a shift of 25 MeV (out of a Q of about 700 MeV) without at the same time significantly affecting the width.<sup>38)</sup> Thus in my opinion the case for identifying the LSM and SFM effects with  $\Lambda_c$  as opposed to for example  $\Sigma(2250)$  rests mainly on the association with electrons. As the reader can judge from Figs. 7 and 8, the statistical significance of the difference in the 2 respective sets of histograms (between  $e^-$  and  $e^+$ ) is quite strong (especially for the SFM data). The charm baryon hypothesis appears the most likely one; the mass question, however, has to be resolved before the issue can be put to rest entirely.

D Production. The SFM group has previously published<sup>21)</sup> evidence for  $D^+$  mesons, as observed in the decay chain  $D^+ \rightarrow K^{*0}\pi^+ \rightarrow K^-\pi^+\pi^+$ . The worrisome features of this result were the large cross section (150–2000 $\mu$ b depending on the model used), strong association with the  $K^*$  in contrast to the SPEAR results, and a slight mass shift: 1.91 GeV observed vs. 1.868 GeV accepted value.

The same group presented at this conference<sup>20)</sup> a preliminary  $4\sigma$  evidence for  $D^0 \rightarrow K^-\pi^+$  at  $\sqrt{s} = 63$  GeV (Fig. 11) observed by using an  $e^-$  trigger. The LSM group presented 95% confidence upper limits for D production from their data with  $K^-$  trigger. Their 2 most stringent limits, the 2 positive D signals, and the result from an older lepton pair ( $e\mu$  and  $ee$ ) experiment<sup>9)</sup> are summarized in Fig. 12. The comparison of the data is

Fig. 11.  $K^-\pi^+$  mass spectrum from the SFM experiment obtained with the  $e^-$  trigger. The smooth curve shows the shape of this spectrum taken with the  $e^+$  trigger.

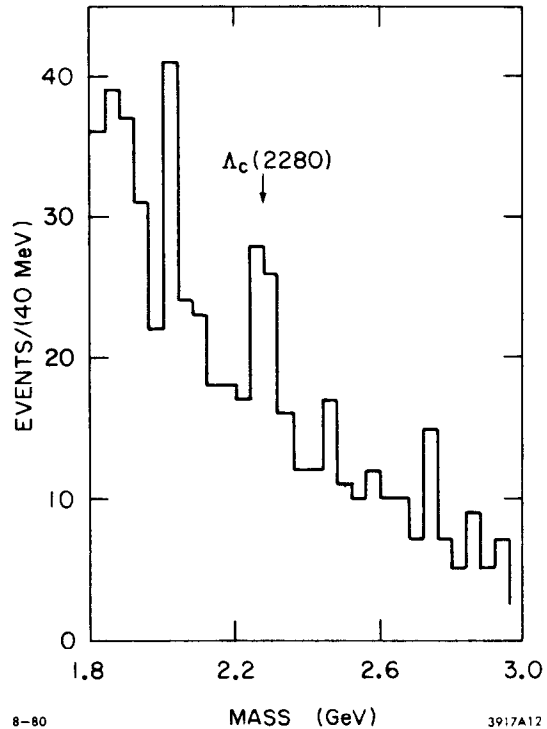
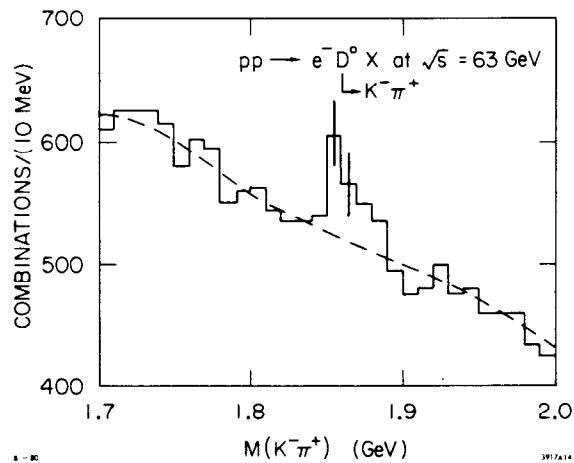


Fig. 10.  $K^0\pi^+$  and  $\Lambda_c^+$  mass spectrum from the  $\nu D$  exposure.



...

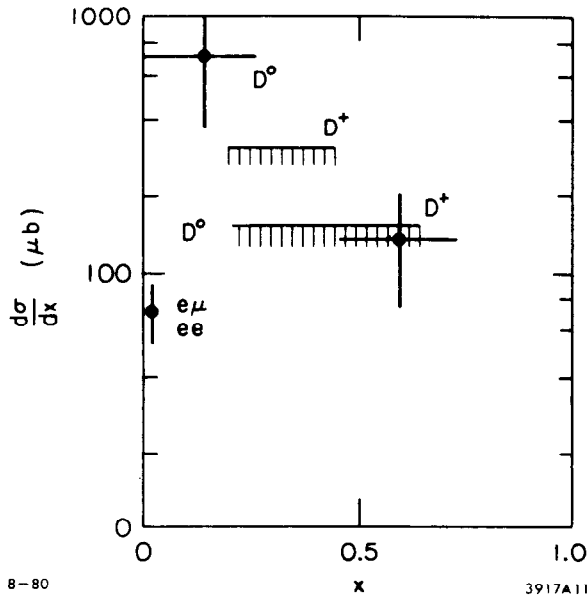


Fig. 12. Summary of the ISR  $D^0$  and  $D^+$  data. The shaded bars correspond to the upper limits from the LSM experiment.

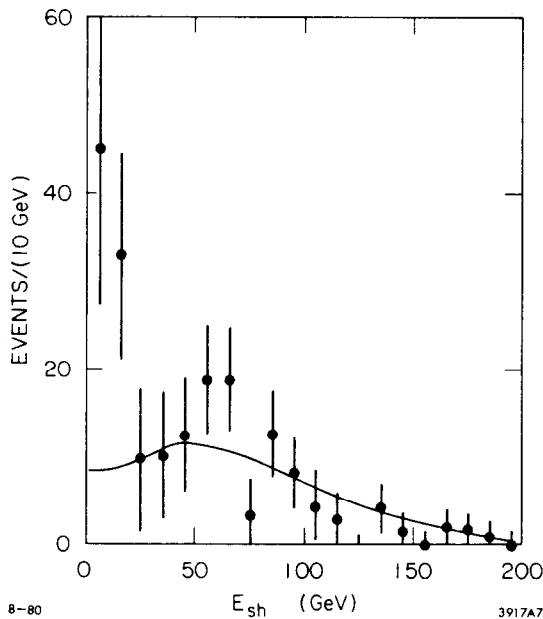


Fig. 13. Visible energy distribution of no- $\mu$  events from CHARM experiment (muon NC events have been subtracted). The curve shows expected contribution to electron neutrino interactions from  $D\bar{D}$  decay.

made difficult by the fact that the semileptonic branching ratios of different charm particles are now known to be quite different.<sup>1,39)</sup> Chilingarov et al., however, assumed 10% BR for both  $D^0$  and  $D^\pm$ . A dominant production of  $D^0(\bar{D}^0)$  near  $x=0$  would be one easy way to resolve the apparent controversy. One should probably end this discussion by noting that the high  $e/\pi$  ratio at low  $x$  and  $p_T$  observed at the ISR<sup>40)</sup> is consistent with the charm production cross section of the order of several hundred microbarns.

3. Anomalies and Discrepancies. I would like to conclude this chapter by discussing 3 experimental results that are either anomalous in themselves or for which different experiments do not give a consistent answer.

a) The CHARM collaboration<sup>19)</sup> in their beam dump experiment sees a  $2.5\sigma$  excess of no- $\mu$  events for shower energies  $2 < E_{sh} < 20$  GeV, above what one would expect from  $D\bar{D}$  production normalized to  $E_{sh} > 20$  GeV (Fig. 13). Specifically the excess is  $54 \pm 19$  (statistical)  $\pm 9$  (systematic) events. Due to instrumental reasons, the other experiments cannot investigate identical region, the closest comparison being with the CDHS experiment who apply a lower cut on shower energy of  $E_{SH} > 5$  GeV. Within  $1\sigma$  their data are consistent (Fig. 14) with the predictions based on  $D\bar{D}$  production.

b) There are some indications that the  $\nu_e/\nu_\mu$  ratio may not be equal to unity. The results of the 3 beam dump experiments are summarized in Table II. That ratio can be obtained either

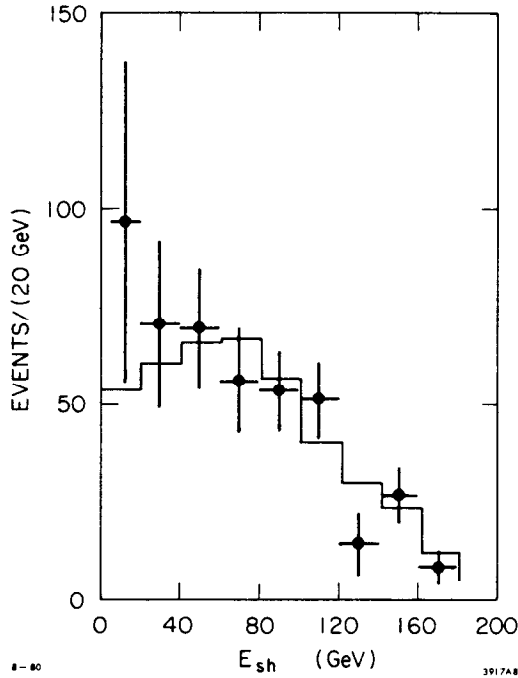


Fig. 14. No- $\mu$  events from CDHS experiment (muon NC events have been subtracted). Solid line indicates prediction from central DD production and decay.

by using prompt  $\nu_\mu$  rate from extrapolation technique (comparison of rates at 2 different densities) or from subtraction method, where one uses a shower cascade calculation to obtain the contribution to  $\nu_\mu$  flux from  $\pi$  and K decay.

One should emphasize here that the systematic errors for the 3 experiments are quite similar and are probably in the direction of overestimating the  $\nu_\mu$  flux (beam scraping or hadronic cascade leakage from the front part of the target would certainly have this effect). The second relevant observation here is that according to the BEBC<sup>25)</sup> and BEBC-TST groups,<sup>41)</sup> this deficiency of  $\nu_e$ 's (if real) cannot be explained on the basis of  $\nu_e \rightarrow \nu_\tau$  oscillations. The conclusion is based on the observation of the expected (within statistical errors) number of  $\nu_e \rightarrow e$  events in the narrow band beam, where the absolute flux of  $\nu_e$ 's is known relatively well.

c) There is a question as to whether the lepton charge ratio is different from unity. The results from both the beam dump experiments and the CIT-Stanford experiment are summarized in Table III.

Table II  
 $\nu_e/\nu_\mu$  Ratios from CERN Beam-Dump Experiments

Group	$\nu_e/\nu_\mu$ Ratio	Statistical Error	Systematic Error	Method
CDHS	0.77	$\pm 0.18$	$\pm 0.24$	Extrapolation
CDHS	0.58	$\pm 0.07$	$\pm 0.19$	Subtraction
CHARM	0.48	$\pm 0.12$	$\pm 0.10$	Subtraction ( $CC\nu_e$ from prod model)
CHARM	0.49	$\pm 0.21$		Extrapolation ( $CC\nu_e$ from prod model)
CHARM	0.44	$\pm 0.11$	$\pm 0.03$	Subtraction ( $CC e$ directly identified)
BEBC	0.59		+0.35 -0.21	Subtraction

Table III  
Lepton charge ratio from different experiments

Group	Ratio	Value	Statistical Error	Systematic Error	Method
CDHS	$\bar{\nu}_\mu/\nu_\mu$	0.12	$\pm 0.20$	$\pm 0.12$	Extrapolation
CDHS	$\bar{\nu}_\mu/\nu_\mu$	0.56	$\pm 0.09$	$\pm 0.13$	Subtraction
CHARM	$\bar{\nu}_\mu/\nu_\mu$	1.3	$\pm 0.5$	+0.4 -0.2	Subtraction
CHARM	$\bar{\nu}_\mu/\nu_\mu$	1.8		$\pm 1.1$	Extrapolation
BEBC	$\bar{\nu}_\mu/\nu_\mu$	0.75		$\pm 0.32$	Subtraction
BEBC	$\bar{\nu}_e/\nu_e$	0.76		$\pm 0.35$	Subtraction
CIT-Stanford	$\mu^-/\mu^+$	1.3		$\pm 0.4$	Extrapolation

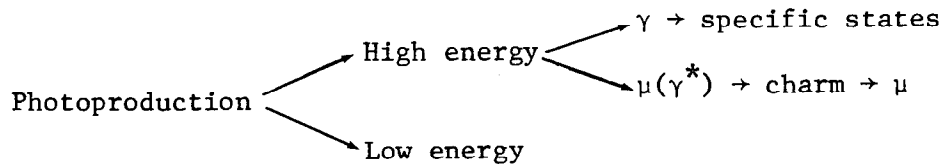
Clearly the largest, and the only really significant departure from unity, occurs for the CDHS extrapolation result. The dependence of the  $\nu_\mu$  and  $\bar{\nu}_\mu$  fluxes on energy is displayed in Fig. 15. Note that this Figure displays observed events, i.e. the ratio of  $\bar{\nu}_\mu/\nu_\mu$  cross sections (0.48) has not been taken out. The discrepancy between the various beam dump experiments is due mainly to the low density  $\mu^+$  point, as can be seen from Fig. 16.

It should be noted that there is nothing fundamental about the charge ratio deviating from unity. A variety of mechanisms, like  $\Lambda_c$  production or unequal  $D^+, D^-$  cross section could alter this ratio either by virtue of different semileptonic branching ratios or different  $x$  dependence.

In summary, several potentially interesting effects are suggested by the data. More detailed experiments are needed, however, to explore and answer these questions.

#### CHARM PRODUCTION BY PHOTONS AND MUONS

We discuss these two topics together since the charm productions by muons occurs via virtual photon mechanism. Thus the physics explored by experiments with these 2 beams is quite similar. Schematically the outline of this chapter can be indicated as follows:



We shall review first the high energy experiments, discussing both the muon experiments that study charm production via their muonic decay modes and the photon experiments, in which specific states are studied via kinematical reconstruction. It is interesting to compare

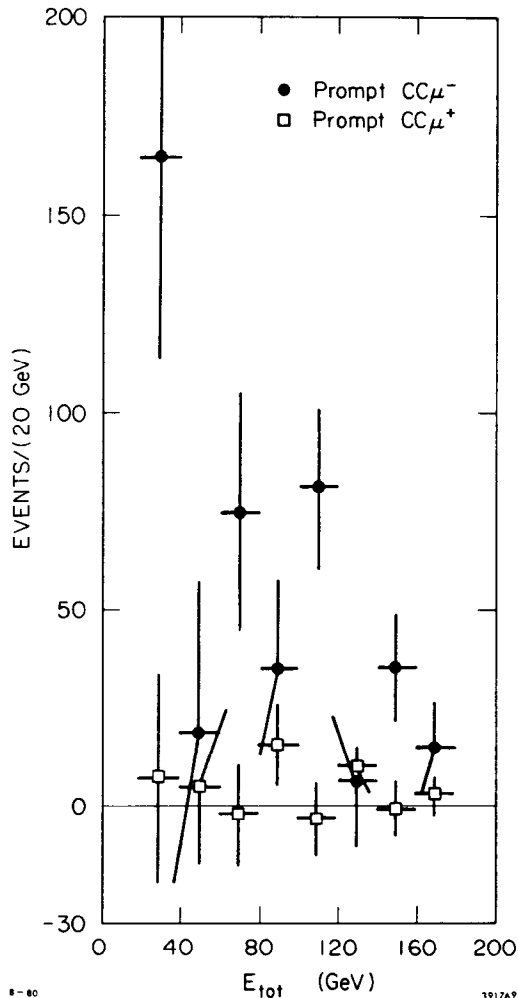


Fig. 15. Prompt  $CC\mu^+$  and  $\mu^-$  spectra from CDHS experiment using the extrapolation method.

emphasize the forward (i.e. diffractive) production region. The results from BFP<sup>45)</sup> can be briefly summarized as follows:

a)  $(81 \pm 10)\%$  of the single extra muon (i.e.  $2\mu$ ) final states are estimated to come from charm production followed by muonic decay of one of the charm particles. The remainder results from the muonic decay of  $\pi$ 's or K's in the hadronic cascade and can be calculated relatively accurately from the available experimental data. The estimated background from this source is shown as inverted histograms in Fig. 17.

b) The data generally show good agreement with the  $\gamma gF$  model as seen from Fig. 17, where the predictions of the model (curves) are compared with the experimental distributions from which the  $\pi$ , K decay background has been subtracted.

the data with the predictions of the photon gluon fusion ( $\gamma gF$ ) model.<sup>42)</sup> This model, based on the lowest order QCD diagram (Fig. 1a) is the QCD analogue of the familiar Bethe-Heitler process, the only difference being the replacement of the virtual photon by a gluon. Thus with one vertex presumably determined by QED, the data can be used to extract the gluon distribution in the nucleon. A useful point of view is to look at this model as predicting a strong correlation between the c and  $\bar{c}$  quarks in the sea, since they originate from the gluon dissociation into a  $c\bar{c}$  pair.

The muon and photon experiments are complementary, in so far that the former are capable of providing very good statistical information at the expense of some of the detail; the latter, on the other hand can study the details of specific charm final states.

The muon data originate from 2 experiments, the Berkeley-Fermilab-Princeton collaboration<sup>43)</sup> (BFP) and the European Muon Collaboration<sup>44)</sup> (EMC). Because of the design meant to specifically emphasize multimMuon final states, the BFP experiment has much better statistics ( $\sim 20072$   $2\mu$  events to be compared with 497 from EMC) and an experimental advantage of absence of any desensitized region in the detector. Both detectors



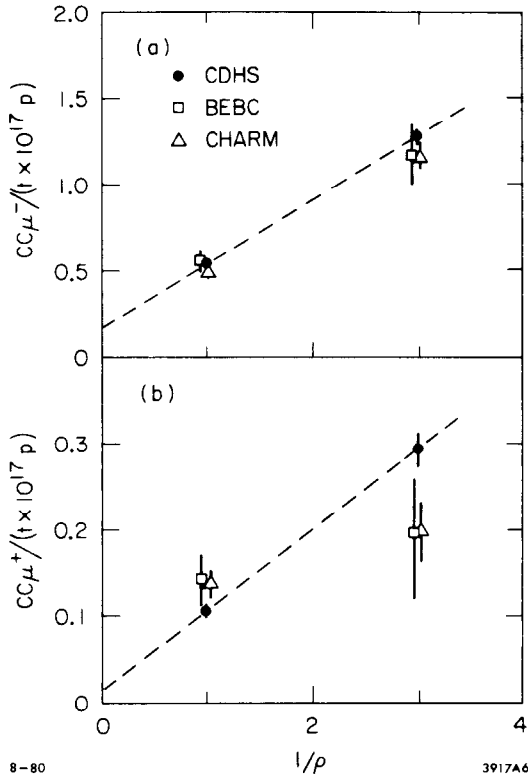


Fig. 16. Comparison of  $CC\mu$  rates as a function of density for the 3 CERN beam dump experiments: a)  $\mu^-$ , b)  $\mu^+$ .

rise, one of which is presumably non-diffractive charm production to which the BFP experiment is insensitive.

Similar conclusions have been reached by the EMC collaboration from the analysis of their  $2\mu$  events.<sup>48)</sup> They have compared their data both to the struck quark model (charmed quark density in the sea taken from the parametrization of Buras and Gaemers<sup>49)</sup>) and to the  $\gamma gF$  model. The first model predicted cross sections about a factor of 5 higher than observed, the latter gave excellent agreement.

The EMC collaboration has also analyzed their  $3\mu$  events with the goal of extracting  $c\bar{c}$  production and their subsequent double muonic decay.<sup>50)</sup> Experimentally, this is a more difficult problem because of the need to eliminate both the electromagnetic trident contribution as well as contributions due to vector meson ( $\rho, \phi, \psi$  etc.)  $2\mu$  decay. These backgrounds can be eliminated to a large extent by two cuts, i.e.

$$1.0 < M_{\mu\mu} < \text{GeV}^2$$

and

$$z < 0.6, \quad \text{with } z \equiv E_{\mu\mu} / \nu.$$

c) The observed diffractive charm production can account for about 1/3 of the total inclusive scale non-invariance in the kinematic region defined by  $2 < Q^2 < 13 \text{ GeV}^2$  and  $50 < \nu < 200 \text{ GeV}$ .<sup>46)</sup>

d) The data appear to require variation of the cross section with the photon energy ( $\nu$ ), as demanded by the  $\gamma gF$  model. Energy independent cross section does not reproduce the data (dashed line in Fig. 17a).

e) Photon charm cross section values have been extracted at two energy intervals, i.e.  $\sigma^\gamma = 750^{+180}_{-130} \text{ nb}$  at  $\bar{E}_\gamma = 178 \text{ GeV}$  and  $\sigma^\gamma = 560^{+200}_{-130} \text{ nb}$  at  $\bar{E}_\gamma = 100 \text{ GeV}$ . The rise with energy is statistically significant,  $\Delta\sigma = 190^{+34}_{-52} \text{ nb}$  because of common systematic errors.

f) It might be interesting to compare these numbers with the total photon hadronic cross section rise of about  $4 \mu\text{b}$  between 40 and 150 GeV.<sup>47)</sup> Of course, other processes are known to contribute also to this

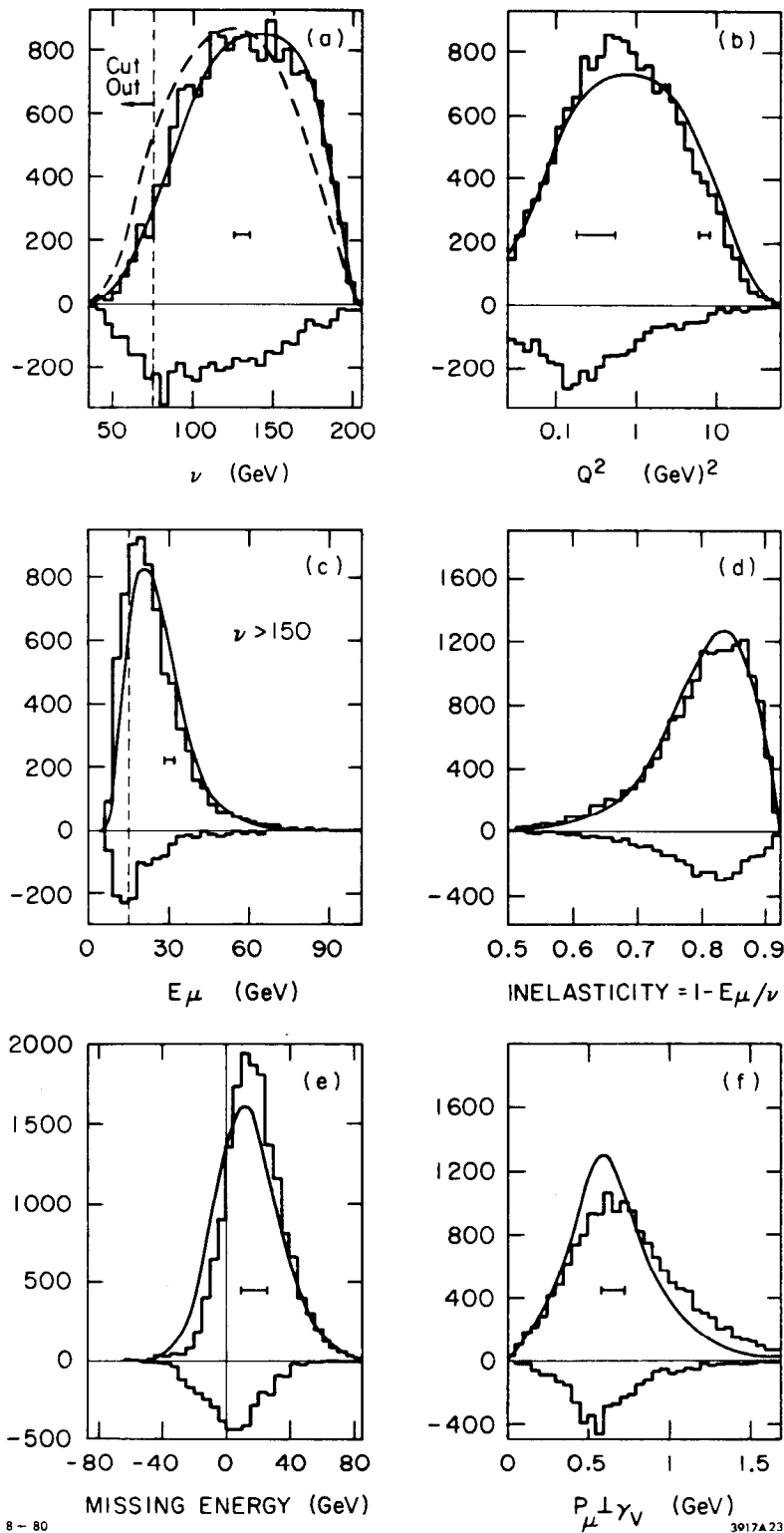


Fig. 17. Comparison of BFP  $2\mu$  data with the predictions of the  $\gamma\gamma F$  model. The inverted histograms show calculated contributions from  $\pi$  and  $K$  decay; the upright ones show the data with that background subtracted.

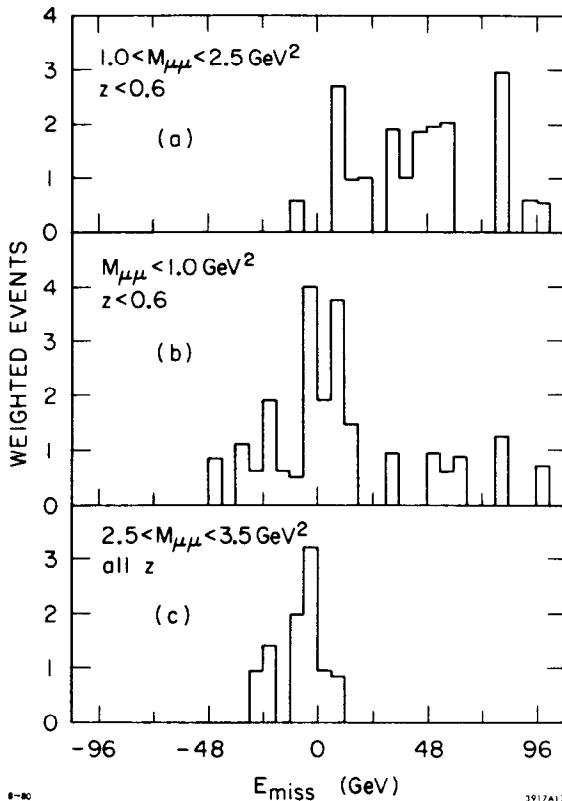


Fig. 18. Missing energy distribution for the 3 different  $M_{\mu\mu}$  ranges from the EMC experiment.

Fermilab collaboration studying charm production by a broadband photon beam. The energy distribution of the beam, acceptance of the apparatus, and charm production cross section are such that most of the data come from events with  $E_\gamma > 80$  GeV. This is very similar to the  $\nu > 75$  GeV cut imposed by the BFP group. The apparatus is also sensitive mainly to the forward production of the charm particles.

Clear signals for  $\Lambda_c$ ,  $\bar{\Lambda}_c$  and  $D^* \rightarrow D\pi$  are seen. The charmed baryons are identified by their  $p(\bar{p})K_S^0$  decay mode (Fig. 20). No significant peak is seen in any other final state with the same quantum numbers. The  $D^* \rightarrow D\pi$  decay chain is identified by looking at the invariant mass difference between a  $K(n\pi)$  and  $K(n-1)\pi$  system where  $n = 2$  or  $3$ . The events with the mass difference in the vicinity of 145 MeV are then candidates for this decay chain. The mass plot of the  $K(n-1)\pi$  system (i.e.  $K^+\pi^\pm$  and  $K_S^0\pi^+\pi^-$ ) for those events shows a clear peak (Fig. 21) at the masses of the  $D^0$  and  $D^\pm$ . In addition, a  $2\sigma$  signal is seen (not shown) for the inclusive  $D^0$  production by looking at  $K^+\pi^\pm$  mass distribution.

The details of the production process again appear to be consistent with the diffractive production of a charm-anticharm pair and can be understood within the framework of the  $\gamma g F$  model. The specific observations that allow one to draw these conclusions are the

The success of these cuts is demonstrated in Fig. 18 where one displays the missing energy distribution. The low mass events, dominated mainly by low mass vector meson and trident contributions, and high mass events, principally  $\psi/J$ , show a missing mass distribution reasonably consistent with zero. The events surviving the cuts, however, show a definite positive value of missing energy,  $E_{\text{miss}} = 44$  GeV indicative of 2 neutrinos accompanying the 2 decay muons. 4 different kinematical quantities from the accepted events are displayed in Fig. 19. Again the fit to  $\gamma g F$  model is very good; the dashed curves show the estimate of the background due to double  $\pi$  and  $K$  decay. The  $\gamma g F$  fit used  $\Lambda = 0.5$  GeV,  $m_c = 1.5$  GeV, and the conventional gluon distribution  $\eta G(\eta) = 3(1-\eta)^5$ .

These data can be compared with the results obtained by the Columbia-Illinois-

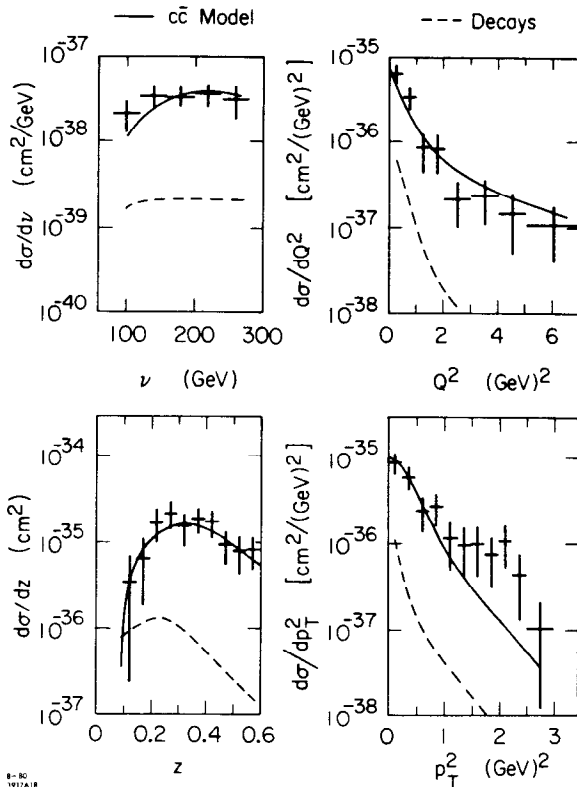


Fig. 19. Comparison of the EMC  $3\mu$  data with the predictions of the  $\gamma F$  model (solid curves). Calculation of background from  $\pi, K$  decays is indicated via dashed curves.

$$\sigma_{\Lambda_c} \approx 200 \text{ nb} \quad (\text{assuming BR for } \Lambda_c \rightarrow K^0 p = 1.5\%)$$

$$\sigma_{D^*} = 160 \pm 70 \text{ nb}$$

$$\sigma_{D^0} = 390 \pm 190 \text{ nb}$$

If we make a reasonable assumption that the relative production rates  $D^0 : D^+ : \Lambda_c : F = 2 : 1 : 1 : 1$  we obtain  $\sigma_{\text{charm}}^{\text{tot}} \approx 1000 \text{ nb}$  at  $\bar{E}_\gamma = 165 \text{ GeV}$ . This number can be compared with BFP value of  $750^{+180}_{-130} \text{ nb}$  at  $\nu = 178 \text{ GeV}$ . We should stress, however, that both experiments are mainly sensitive to the forward production region.

The production mechanisms appear to be quite different at lower energies. The WA4 experiment at CERN has studied<sup>52)</sup> the photoproduction of charm particles using a tagged photon beam with  $E_\gamma < 70 \text{ GeV}$  and the  $\Omega$  apparatus that has considerably larger acceptance at wide angles than the CIF spectrometer. The most relevant features of their observations can be summarized as follows:

following:

- a)  $\Lambda_c$  and  $\bar{\Lambda}_c$  production cross sections are equal.
- b) Charmed baryon appears to take about half of the  $\gamma$  ray energy:  $\bar{E}_{\Lambda_c} / \bar{E}_\gamma = 0.52$ .
- c) The numbers of observed  $D^{*+}$  ( $61 \pm 14$ ) and of  $D^{*-}$  ( $65 \pm 15$ ) are equal within errors.
- d) The  $D$  signal appears only in association with a  $K$  of opposite sign i.e. there is a  $K^-\pi^+$  peak at the mass of the  $D^0$  if a  $K^+$  is identified elsewhere in the event. No signal is seen in association with a proton or antiproton, or  $K$  of the same sign.

Finally we can say a word about cross sections. The data are insufficient to say anything about the energy dependence in the region under study. For the purpose of extracting numbers, cross section was assumed to be flat over the whole energy range covered by the experiment. The deduced cross sections for the specific channels are:

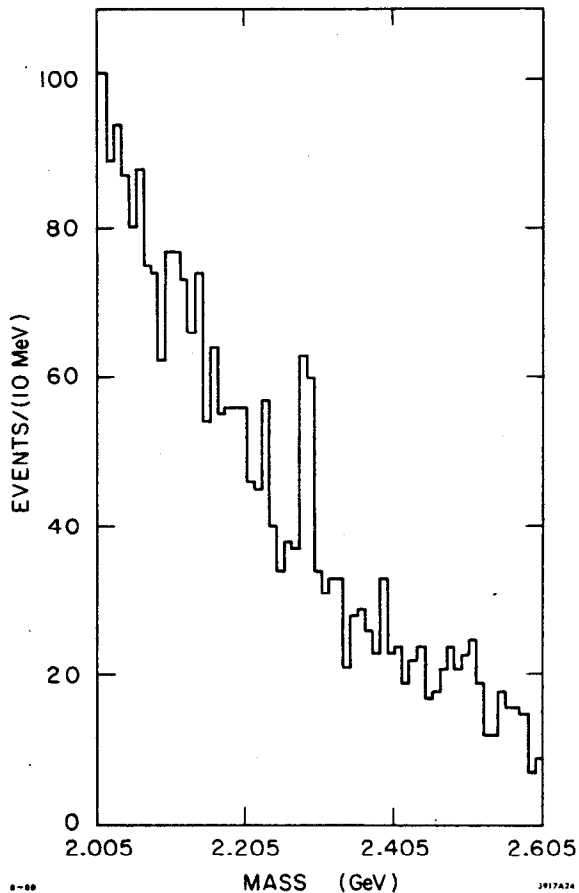


Fig. 20.  $pK_S^0$  and  $\bar{p}K_S^0$  mass spectrum from the CIF experiment.

best estimate for the F mass is  $M_F = 2.020 \pm 0.010$  GeV. One should add here that of the 3 identified F decays in emulsions,<sup>53)</sup> none is associated with an  $\eta$ . Thus  $\eta + \pi$ 's decay modes probably do not constitute more than 50% of the total decays implying a reasonably large F photoproduction cross section of about 200 nb.

Table IV  
Summary of the  $F \rightarrow \eta + \pi$ 's observations

Mode	Width Expected	(MeV) Observed	Observed Mass (GeV)	Efficiency	$B\sigma$ (nb)
$\eta\pi$	75	$108 \pm 31$	$2.047 \pm .025$	.07	$12 \pm 3$
$\eta 3\pi$	50	$38 \pm 24$	$2.021 \pm .015$	.10	$60 \pm 15$
$\eta' 3\pi$	40	$48 \pm 34$	$2.008 \pm .020$	.05	$20 \pm 8$

a) A statistically significant  $\bar{D}^0$  peak is observed in  $K^+\pi^-$  and  $K^+\pi^-\pi^0$  spectra but no comparable peak is seen for the charge conjugate states (Fig. 22).

b) This enhancement becomes especially pronounced when one looks only at the events with an associated proton (Fig. 23a). Similarly the  $K_S^0\pi^+\pi^-$  (Fig. 23b) and  $K_S^0\pi^-\pi^0$  combinations peak at the  $D^0$  mass if one demands a similar association with the proton. Thus the natural explanation is the charm production via an associated production mechanism  $\gamma p \rightarrow \Lambda_c \bar{D}$ ,  $\Lambda_c$  subsequently decaying to a proton. No statistically significant enhancement at the  $\Lambda_c$  mass is seen however in any  $(\Lambda\pi)$ 's,  $(Kp\pi)^+$ , or  $K^0p$  combination.

c) There is evidence for F's in  $\eta + \pi$ 's channels (Fig. 24). The  $\eta$ 's are identified by their  $2\gamma$  decay mode. The majority of the F signal in the  $\eta 5\pi$  system appears to come from the  $\eta' 3\pi$ . The parameters of the F observations are summarized in Table IV. The

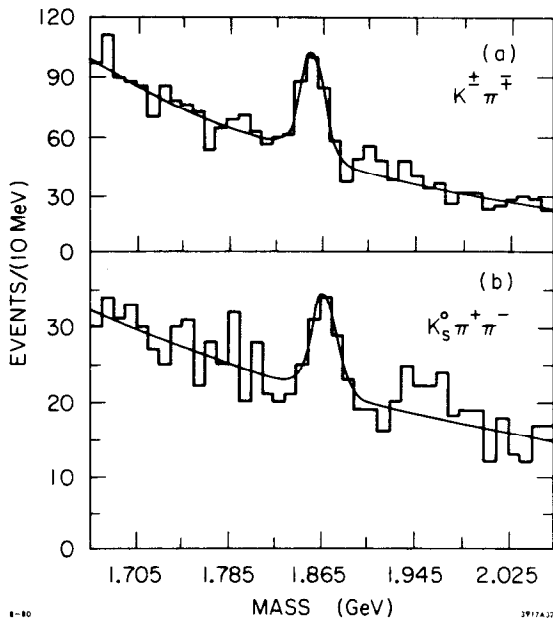


Fig. 21.  $K^\pm\pi^\mp$  and  $K_S^0\pi^+\pi^-$  mass spectra from the CIF experiment for events with  $M_{K3\pi} - M_{K2\pi}$  (or  $M_{K2\pi} - M_{K\pi}$ ) around 145 MeV.

the lower energy range the associated production of CD in the central

d) The following cross section estimates have been extracted from the data (I summarize here only the most significant ones).

$$\sigma(\gamma p \rightarrow \bar{D}^0 X) = 515 \pm 160 \pm 100 \text{ nb}$$

$$\sigma(\gamma p \rightarrow D^0 X) < 450 \text{ nb } 3\sigma \text{ level}$$

$$\sigma(\gamma p \rightarrow C\bar{D}^0 X) = 510 \pm 220 \text{ nb}$$

$$\sigma(\gamma p \rightarrow CD^- X) = 450 \pm 310 \text{ nb}$$

(in the last 2 estimates C stands for any charmed baryon, one assumes central production, and branching ratio  $C \rightarrow p + X$  of 50%).

e) The inclusive  $\bar{D}^0$  cross section has also been evaluated as a function of energy. It appears to rise steeply over the explored range of  $20 < E_\gamma < 70 \text{ GeV}$  (Fig. 25).

In conclusion we can say that the charm photoproduction appears to be dominated by different mechanisms in the different energy regions. In

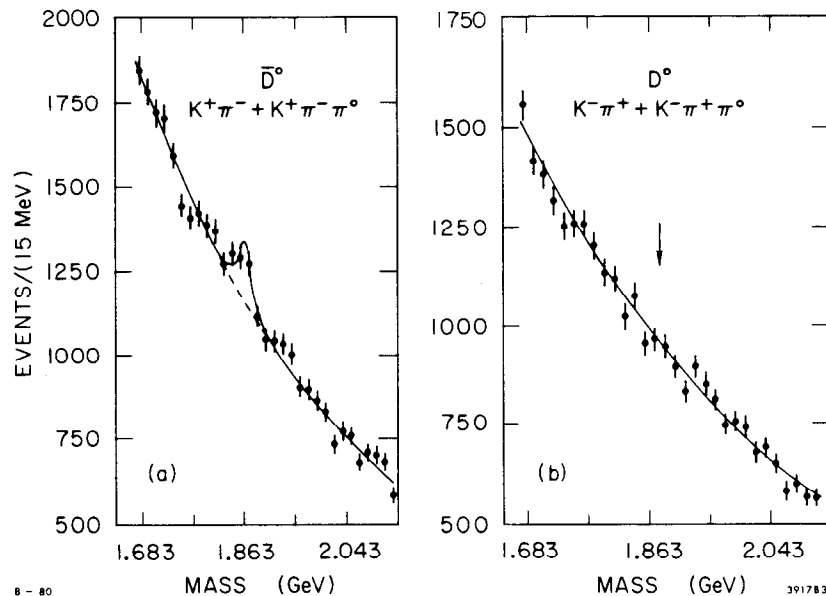


Fig. 22.  $K^+\pi^-$  and  $K^+\pi^-\pi^0$  (a) and  $K^-\pi^+$  and  $K^-\pi^+\pi^0$  (b) mass spectra from the WA4 experiment.

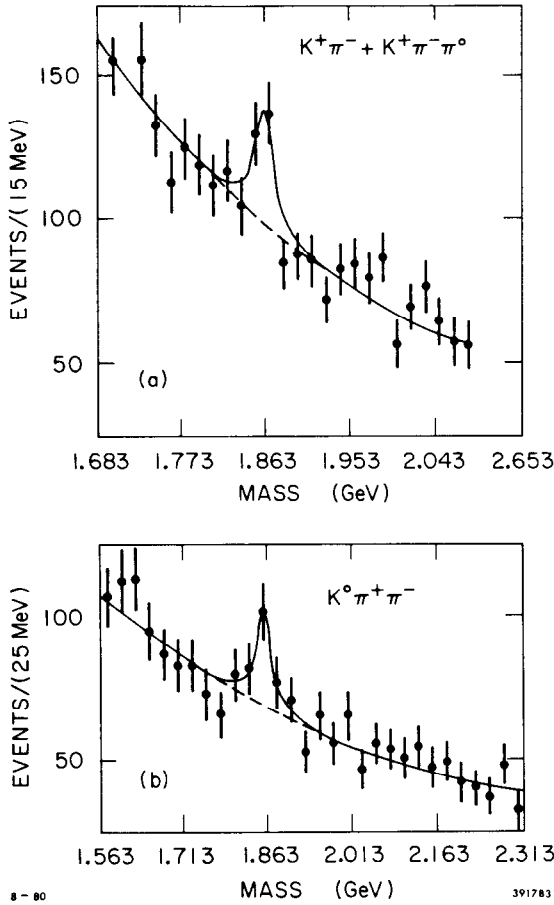


Fig. 23.  $K^+\pi^-$  and  $K^+\pi^-\pi^0$  (a) and  $K^0\pi^+\pi^-$  (b) mass spectra from the WA4 experiment for the events in association with a proton.

the poor acceptance of the CIF spectrometer for this process. One should add here that the preliminary results from the FRAMM collaboration<sup>54)</sup> working at medium energies support the diffractive production mechanism although their trigger and event selection criteria strongly bias them in that direction. On the other hand the only fully reconstructed emulsion event of charm photoproduction<sup>55)</sup> is an example of associated production with  $E_\gamma = 25$  GeV. Finally, the Vector Meson Dominance hypothesis makes predictions about the ratio of elastic  $\psi$  to open charm photoproduction.<sup>56)</sup> The results of the BFP group would imply that non diffractive charm production must be at least comparable in magnitude to the diffractive production.

#### NEW FLAVOR PRODUCTION BY NEUTRINOS

It has been only 6 years ago since the HPWF group reported at the London conference observation of  $2 \mu^+\mu^-$  events from neutrino interactions.<sup>57)</sup> This first indication of charm production was the beginning of an intensive effort in this field which has led to the

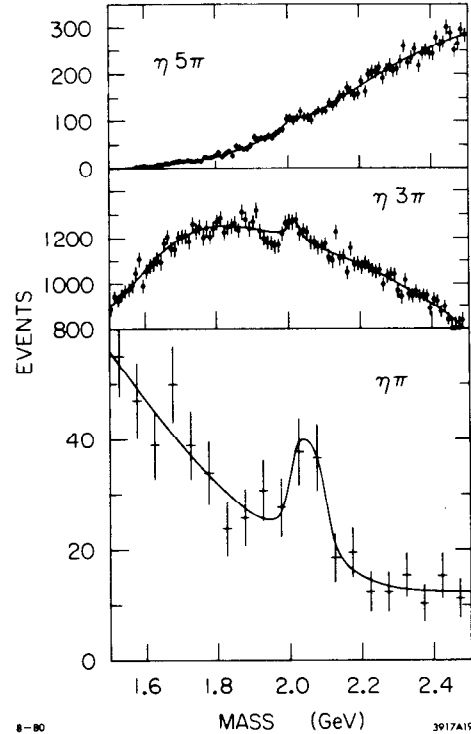


Fig. 24. Mass spectra of the  $\eta + n\pi$  systems from the WA4 experiment.

region appears predominant; at higher energies the diffractive mechanism appears to take over. The amount of associated production at higher energies is uncertain because of

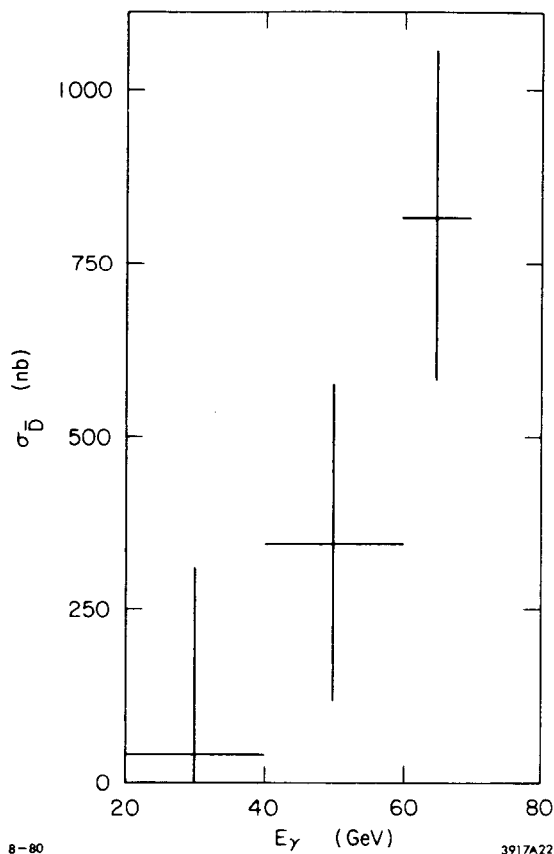


Fig. 25.  $\bar{D}^0$  cross section as function of energy from WA4 experiment.

on dimuon events as a function of neutrino energy is displayed in Fig. 26. We see that the ratio of  $(\mu^+\mu^+)/\mu^+\mu^-$  is reasonably constant at about 0.1; in addition the rate of dimuon events is about an order of magnitude higher than the prediction based on associated charm production using a first order QCD diagram.<sup>62)</sup>

Two contributions on same sign  $\mu e$  events have been received at this conference. The BFHWW collaboration<sup>63)</sup> quotes an upper limit on  $\mu^-e^-/\mu^- < 5 \times 10^{-4}$  from  $\bar{\nu}$  interactions, based on observation of 4  $\mu^-e^-$  events with a calculated background of 4 events. The cut on electron momentum is  $P_e > 4$  GeV. 4  $\mu^+e^+$  events have been observed by the IFIM collaboration in  $\bar{\nu}$  interactions ( $P_e > 0.4$  GeV and expected background of 0.8 events) giving a ratio of  $\mu^+e^+/\mu^+ = (6.4^{+3.6}_{-2.4}) \times 10^{-4}$ . A very interesting feature of these events is that 3 of them are associated with a  $V^0$  ( $2\Lambda$ 's and 1  $K_S^0$ ). The IFIM point is also displayed in Fig. 26 but it should be mentioned that it is not directly comparable to the  $\mu\mu$  points since the electron momentum cut is considerably lower than the typical muon cut (generally  $p_\mu \geq 9$  GeV).

The leptons of the same sign could be an indication of associated charm production with a rate considerably higher than expected on the naive grounds, a first evidence of new flavor production in neutrino interactions, or presence of as yet unexpected new

presentation at this conference by the CDHS group of results based on some 10000  $\mu^+\mu^-$  events.<sup>58)</sup> Such large statistics allow one to study in detail the structure function of the strange sea and the results of this analysis have been presented in Sciulli's rapporteur talk. In this review, I shall concentrate solely on the neutrino production of lepton pairs of the same sign, as this process might be an indication of a production mechanism that is also relevant in photon and hadron processes.

First evidence for dimuon events of like sign has been published already some time ago.<sup>59)</sup> At this conference extensive new data on this channel has been presented by the CFNRR collaboration;<sup>60)</sup> in addition some first positive evidence for  $\mu e$  events of some sign has been presented by the IFIM collaboration<sup>61)</sup> studying  $\bar{\nu}$  interactions in the 15' BC at Fermilab. The data



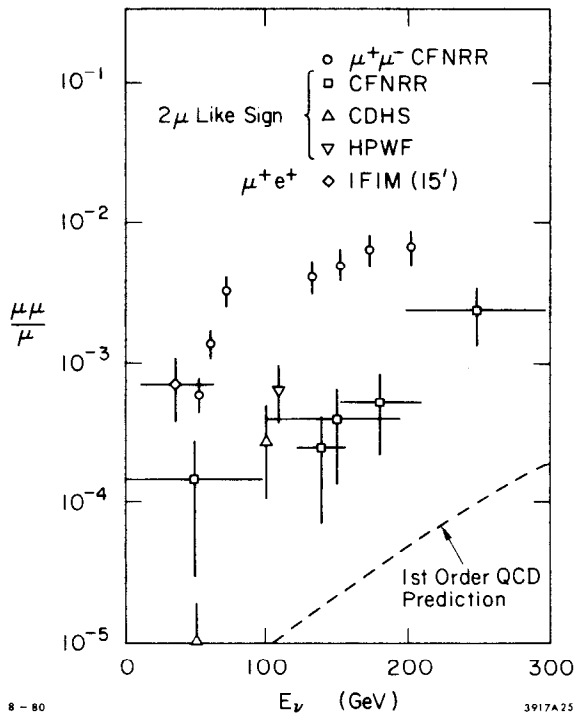


Fig. 26. Summary of like dilepton data from the neutrino interactions. CFNRR points for  $\mu^+\mu^-$  are also shown for comparison. The curve is 1st order QCD prediction (ref. 62).

This limit, obtained from 185 GeV  $\pi^-$  interactions, can be compared

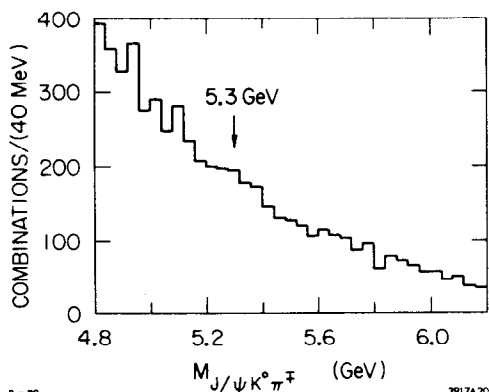


Fig. 27. Mass spectrum of the  $J/\psi K^0\pi^{\mp}$  system from the WALL experiment.

phenomenon. More detail and better statistics will be necessary to resolve this question.

#### STATUS OF HEAVIER FLAVORS

A year ago there was presented a preliminary evidence<sup>64)</sup> for the production of a bottom meson decaying via  $B \rightarrow \psi K\pi$ . The WALL group has now increased their statistics fourfold to about 40000  $J/\psi$  events and find that the peak has disappeared<sup>65)</sup> (Fig. 27). These data and  $\psi K^0$  mass plot (not shown) give upper limits on these 2 decay modes i.e.

$$\sigma_{\overline{B}B} \cdot \text{BR}(B \rightarrow J/\psi K^0\pi^{\pm}) < 0.51 \text{ nb/nucleon}$$

$$\sigma_{\overline{B}B} \cdot \text{BR}(B \rightarrow J/\psi K^0) < 0.08 \text{ nb/nucleon}$$

There have been estimates<sup>66)</sup> that the first decay mode should have a branching ratio of about 1%, which would translate into a total production upper limit of  $\sigma_{\overline{B}B} < 51 \text{ nb}$ .

compared with upper limits obtained using different techniques from 2 other experiments. The Princeton-Chicago group,<sup>67)</sup> have obtained  $\sigma_{\overline{B}B} \cdot \text{BR}(B \rightarrow J/\psi + X) \leq 0.24 \text{ nb/nucleon}$  for 225 GeV  $\pi^-$  interactions. This limit is very sensitive to the  $B \rightarrow \mu$  branching ratio (assumed to be 18%) as the experiment involves search for  $J/\psi$  in association with a high  $p_T$  muon. A reasonable assumption of 3% BR for the  $J/\psi + X$  inclusive decay mode would translate the result into an upper limit of  $\sigma_{\overline{B}B} < 8 \text{ nb}$ . Finally, the Cal Tech-Stanford experiment<sup>68)</sup> has set a limit of  $\sigma_{\overline{B}B} < 50 \text{ nb}$  for 400 GeV proton interactions by looking for a variety of multimuo final states. These numbers should be compared

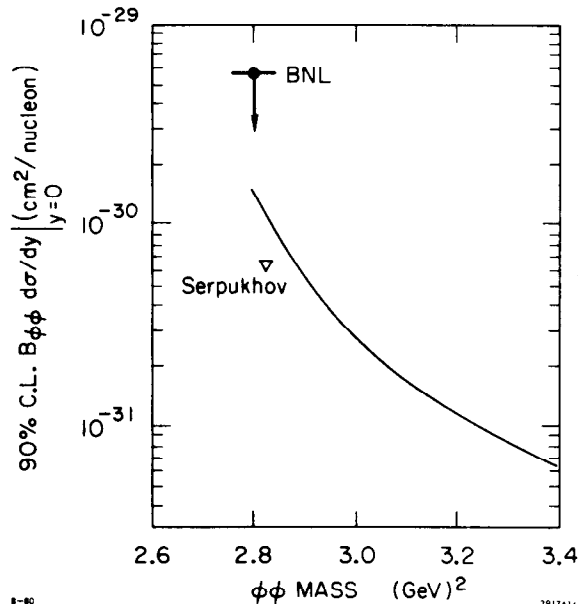


Fig. 28. Upper limits (as a function of  $\eta_c$  mass) for  $B(\eta_c \rightarrow \phi\phi) \frac{d\sigma}{dy} \Big|_{y=0}$  obtained by the Fermilab-Stonybrook collaboration.

results from Brookhaven ( $\pi^-p \rightarrow \phi\phi n$ ) and Serpukhov ( $\pi^-p \rightarrow \gamma\gamma n$ ) experiments, scaled to the Fermilab energy region. Lipkin<sup>71)</sup> has suggested that  $\sigma \cdot BR(J/\psi \rightarrow e^+e^-) \approx \sigma \cdot BR(\eta \rightarrow \phi\phi)$ . That would make  $10^{-32} \text{ cm}^2$  an interesting goal to strive for. In addition, a low energy BNL experiment<sup>71)</sup> (13 GeV) reported at this conference a limit of 260 pb for  $\sigma \cdot BR$  for the process  $\pi^-p \rightarrow \eta_c n$ ,  $\eta_c \rightarrow \gamma\gamma$ .

b) T muonproduction. The BFP group presented<sup>72)</sup> an upper limit for T production via 208 GeV/c muons. Their 90% CL number for the process  $\sigma(\mu N \rightarrow \mu TN)B(T \rightarrow \mu^+\mu^-)$  is  $2.2 \times 10^{-38} \text{ cm}^2$  to be compared with the prediction of the  $\gamma$ GF model of  $(4.0 \pm 1.2) \times 10^{-39} \text{ cm}^2$ .

c) J/ $\psi$  and T hadroproduction. The data for these processes are now becoming quite extensive and allow rather detailed comparisons with various phenomenological models. I shall limit myself here to describing some very general features of these reactions which have a bearing on various production mechanisms. Specifically, I shall summarize the cross section data for various beams, the x dependence, information on intermediate states, and the decay angular distributions.

Additional total cross sections measurements for  $x_F > 0$  for J/ $\psi$  and T production by pions have been reported by the NA3 collaboration.<sup>73)</sup> Together with the older measurements they are displayed as  $M^2\sigma$  in Fig. 29. For comparison, I have also included lines indicating the approximate dependence of the same variable in the proton induced reactions.

The dependence of the cross section on the nature of the incident beam is interesting because it sheds light on the relative importance of the quark-antiquark vs. gluon-gluon fusion mechanisms. Naively,

with a first order QCD prediction of a cross section in the neighborhood of a few nanobarns.

#### PRODUCTION OF BOUND FLAVORS

From the phenomenological point of view, the bound heavy flavor states are made by the same kind of diagrams as the unbound states. The fundamental difference is that the integration over the effective mass of the  $c, \bar{c}$  quark pair cuts off at  $2 m_D$  (for charm states) and that certain diagrams are forbidden if all the relevant quantum numbers are to be conserved (J,P,C).

a)  $\eta_c$  search. There still is no evidence for production of  $\eta_c$  outside of  $e^+e^-$  annihilations. A search at Fermilab using the decay mode  $\eta_c \rightarrow \phi\phi$  has yielded negative results.<sup>69)</sup> The limits as a function of mass are displayed in Fig. 28 together with earlier results

3912A6

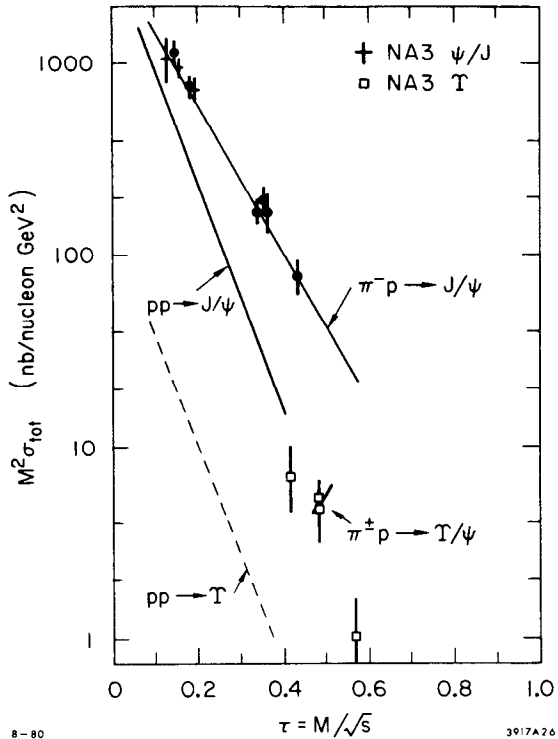


Fig. 29. Cross section for  $J/\psi$  and  $T$  production in  $\pi$  nucleon interactions plotted in terms of scaling variables. For comparison, lines corresponding to production by protons are also shown.

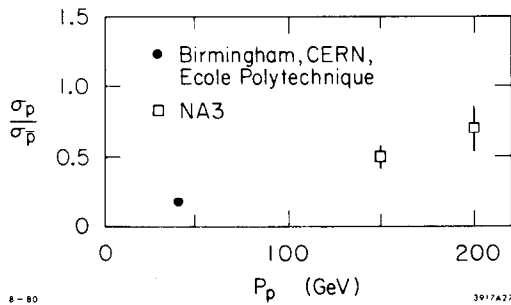


Fig. 30. Ratio of  $\sigma(pN \rightarrow J/\psi + X) / \sigma(\bar{p}N \rightarrow J/\psi + X)$  as a function of incident energy.

is quite poor and should be contrasted with the situation in Fig. 31c,d,e where the data were fitted to the gluon-gluon fusion mechanism assuming for the gluons the functional form

because of the relationship  $M^2 = s x_1 x_2$ , we would expect the gluon production mechanism to become more important at higher energy, since the gluon spectrum is rather soft. Furthermore, at lower energies,<sup>74)</sup> where  $q\bar{q}$  fusion might dominate, the cross sections for beams of particles containing appropriate valence antiquarks would be expected to be higher than for the particles without such valence quarks. These features are indeed demonstrated by the data shown in Fig. 30 where we plot the ratios for  $J/\psi$  production in the proton and antiproton beams. For gluon fusion dominance the  $\sigma_p/\sigma_{\bar{p}}$  ratio should approach unity. These qualitative features are also demonstrated in  $J/\psi$  production by 40 GeV K beams where we have  $\sigma_{K^+}/\sigma_{K^-} = 0.29 \pm 0.07$  and in the relative production of  $T$  by  $K^+$  and  $\pi^+$  beams<sup>75)</sup> at 200 and 280 GeV where  $\sigma_{K^+}/\sigma_{\pi^+} = 0.10$ . Note that the valence antiquark in  $K^+$ , i.e.  $\bar{s}$ , cannot annihilate with any valence quark in the nucleon to give a  $J/\psi$  or an  $T$ . As might be expected, the  $\pi^+$ - $\pi^-$  ratio for  $J/\psi$  production is consistent with unity.

The importance of the gluon mechanism in 150 GeV  $\pi^-p$  interactions is demonstrated by the analysis<sup>76)</sup> of the  $x_F$  distribution of the  $J/\psi$ . This distribution should be determined entirely by the pion and nucleon structure functions if  $q\bar{q}$  annihilation is dominant. The data are compared to the theoretical expectations in Fig. 31a,b where NA3 structure functions have been used in calculating the expected curves. The agreement

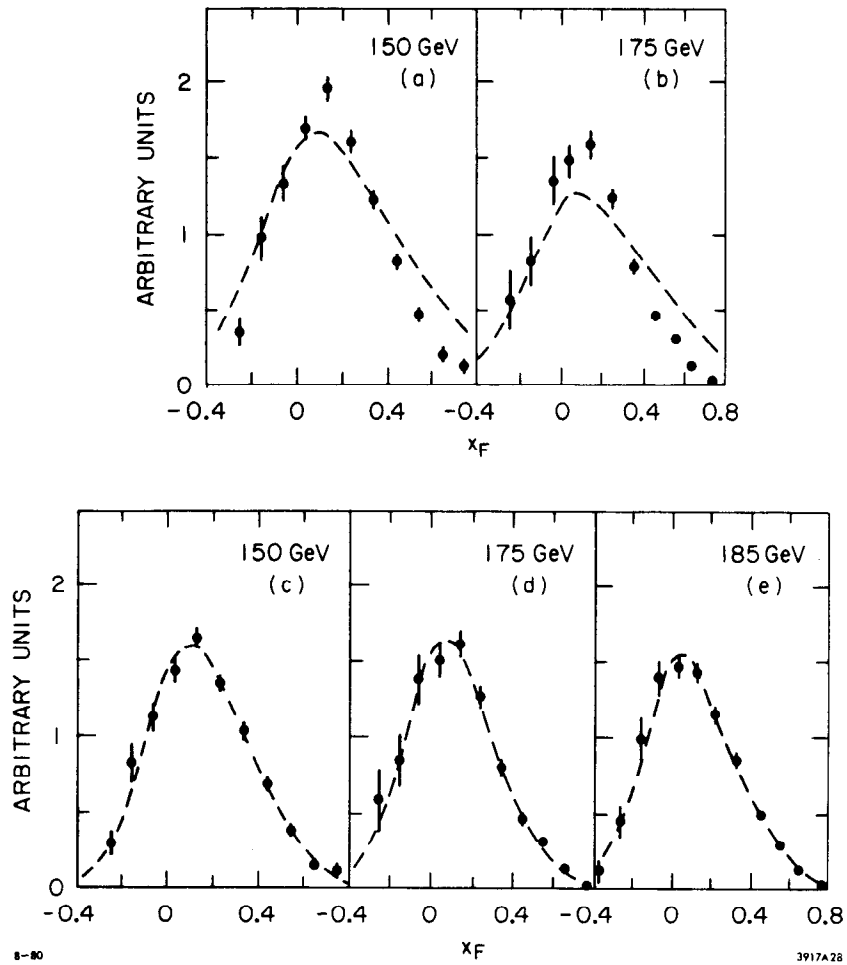


Fig. 31.  $x_F$  distribution for  $J/\psi$  production (points) from the Wall experiment at different energies compared to quark-quark fusion prediction (a and b) and gluon-gluon fusion fits (c,d,e).

$$\eta g_{\pi}(\eta) \sim (1-x)^m$$

$$\eta g_N(\eta) \sim (1-x)^n$$

The fits gave very reasonable values of  $m = 2.3 \pm 0.3$  and  $n = 5.1 \pm 0.6$  and appear to reproduce the data quite well.

The same collaboration has also searched<sup>77)</sup> for  $\gamma$  rays associated with the  $J/\psi$  production. 2 experimental techniques were used to look for the photons: a Pb/scintillator sandwich calorimeter with a mean energy resolution of  $50\%/\sqrt{E}$  FWHM and a  $\gamma \rightarrow e^+e^-$  conversion (22 MeV FWHM) either in the Be target or in downstream scintillators and chambers. Both methods give evidence for an intermediate  $\chi$  state: the calorimeter shows 1 broad unresolved peak (Fig. 32a) in the  $J/\psi$   $\gamma$  mass spectrum between 3.5 - 3.6 GeV which corresponds to  $36 \pm 5\%$  of the  $\psi$ 's resulting from the  $\chi$  decay. The conversion technique gives

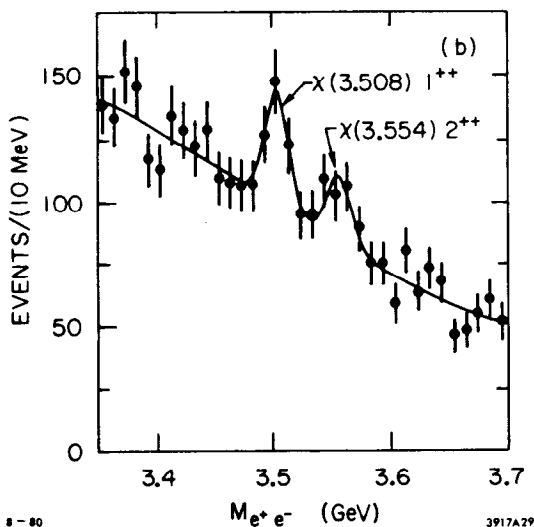
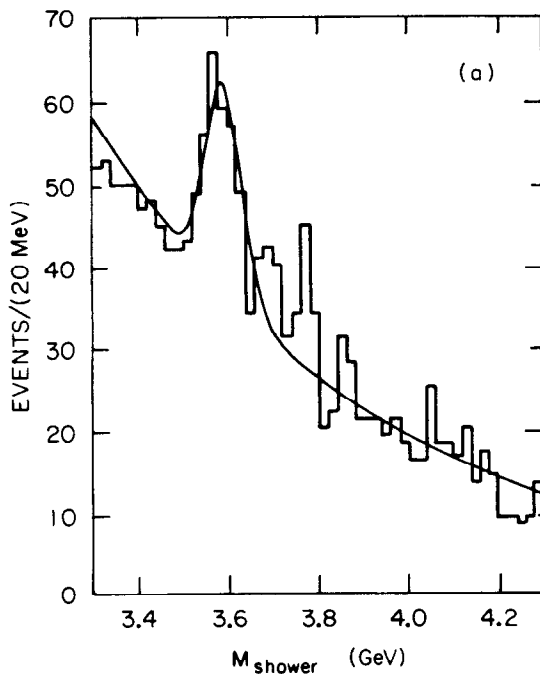


Fig. 32. Mass spectrum of the  $J/\psi + \gamma$  system from the WALL experiment using a calorimeter (a) and spectrometer (b).

dominant mechanism being gluon-gluon fusion, the growth in importance of that mechanism with increasing energy, and an appreciable fraction of the  $J/\psi$  produced via an intermediate  $\chi$  state.

d)  $J/\psi$  muoproduction. Partial results on this process have been published previously by both the BFP<sup>78)</sup> and EMC<sup>79)</sup> groups. In general the total cross section for this process, when extrapolated to  $Q^2 = 0$  appears to agree quite well with the lower energy

two distinct peaks in this region (Fig. 32b): the first one identified with the  $1^{++} \chi$  (3.508) and corresponding to  $19 \pm 4\%$  of all  $J/\psi$  events, and the second with  $2^{++} \chi$  (3.554) and accounting for  $12 \pm 4\%$  of all events. Using the known branching ratios for  $\chi \rightarrow J/\psi + \gamma$  decay, these numbers correspond to a production cross section ratio of

$$\sigma_{2^{++}} / \sigma_{1^{++}} = 1.4 \pm 0.9.$$

The results of the calorimeter and conversion techniques are consistent with each other because of much different resolving power of the 2 methods. The total fraction of  $J/\psi$  proceeding via  $\chi$  intermediate state ( $\sim 35\%$ ) is consistent with other measurements both at Fermilab and at the ISR.

The decay angular distribution of the  $J/\psi$  has been studied<sup>73)</sup> by the NA3 collaboration for  $\pi^-$  production at 150 GeV. The most general distribution has to be of the form

$$\frac{dN}{\cos\theta} = 1 + \lambda \cos^2\theta.$$

For direct light quark annihilation  $\lambda$  has to be near unity. The experimentally observed value  $\bar{\lambda} = 0.05 \pm 0.07$  is consistent with previous measurements and argues that either quark annihilation proceeds via an intermediate state or is not a very important process at this energy.

In conclusion, the overall picture is consistent with the picture is consistent with the

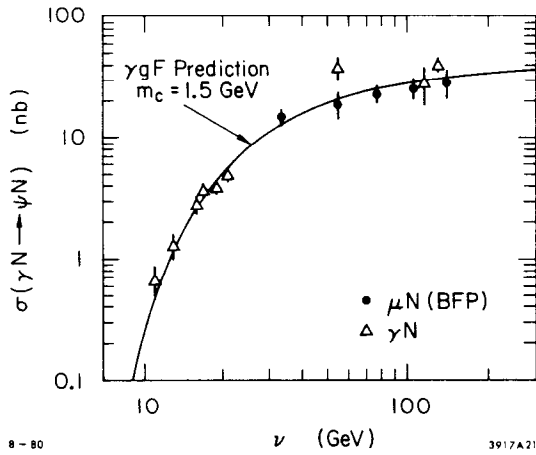


Fig. 33. Comparison of BFP  $J/\psi$  muoproduction points (extrapolated to  $Q^2 = 0$ ) with the photon points and predictions of the  $\gamma\gamma F$  model (ref. 80).

$$W(\theta, \phi) = \frac{1 + \cos^2\theta + 2\varepsilon R \sin^2\theta - \varepsilon\eta \sin^2\theta \cos 2\phi}{(1 + \varepsilon R) (1 + Q^2/\Lambda_{\text{eff}}^2)^2}$$

Where  $\varepsilon$  gives the ratio of longitudinal to transverse photon flux ( $\bar{\varepsilon} = 0.8$  for BFP data),  $R = \sigma_L/\sigma_T$ , and  $\eta = 1$  if S-channel helicity is conserved and we have natural parity exchange.  $R$  was parametrized as either constant or linear in  $Q^2$  and data were fitted to  $\eta$  and  $\Lambda_{\text{eff}}$ . The following conclusions can be reached from the fit:

1 - s channel helicity conservation and natural parity exchange appear to be valid, i.e.  $\psi$  "remembers" photon helicity.

2 - independent of assumptions about  $R$ ,  $\Lambda_{\text{eff}}$  is significantly smaller than  $m_\psi$ , typical value being  $2.15^{+0.19}_{-0.13}$  GeV. This can be compared with the published EMC value<sup>79)</sup> of  $2.4 \pm 0.3$  GeV obtained by fitting their data to  $C(1 + Q^2/\Lambda_{\text{eff}}^2)^{-2}$ ,  $C$  and  $\Lambda_{\text{eff}}$  being free parameters.

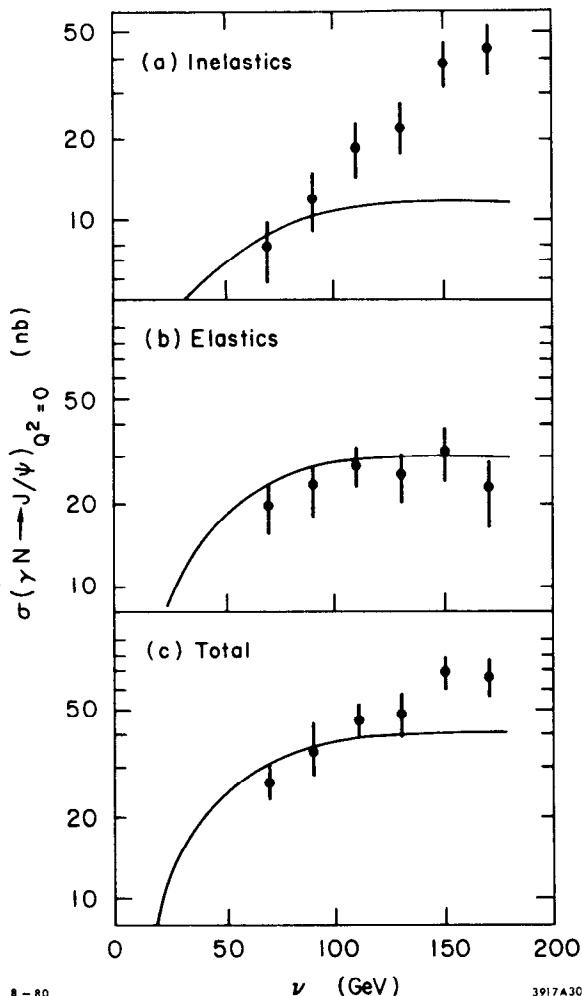
3 - when  $R$  is allowed to vary linearly with  $Q^2$ , i.e.  $R = \xi^2 Q^2 / m_\psi^2$ , the best fit yields  $\xi^2 = 4.6^{+4.8}_{-3.8}$ .

The European Muon Collaboration has presented results<sup>81)</sup> on inelastic  $J/\psi$  production with a total cross section approximately equal to that of the elastic  $J/\psi$  production. The inelastic events are defined as ones having more than 5 GeV deposited in the target. Those events tend to peak at high  $\nu$  (Fig. 34) and have much broader  $p_T^2$  distribution than the elastic events.

An effort has been made to estimate the contribution to these events from the production of higher lying bound charmonium states ( $\psi'$  and  $\chi$ ). The different methods indicate that only about half of the inelastic events come from that source. Their  $z$  distribution would tend to peak near high values in agreement with the data and the  $\nu$  dependence can be calculated using the  $\gamma\gamma F$  model (Fig. 34b). It appears that the large fraction of events with  $\nu > 100$  GeV must

photoproduction experiments and the  $\gamma\gamma F$ .<sup>80)</sup> The comparison of the photon data with the BFP results is shown in Fig. 33; the EMC results from 280 GeV muon run also fall on the drawn curve.

To study the details of the  $J/\psi$  muoproduction the BFP group has performed a 3 dimensional fit<sup>45)</sup> in  $\theta, \phi$ , and  $Q^2$ , where  $\theta$  is the polar angle of  $\mu^+$  relative to  $J/\psi$  and  $\phi$  is the angle between the lepton scattering plane and  $\psi$  decay plane, both angles being defined in the helicity frame. The data were fitted to



8-80

3917A30

Fig. 34.  $\nu$  distribution of elastic and inelastic  $J/\psi$ 's from the EMC collaboration. The curves are predictions of the  $\gamma F$  model (higher lying charmonium states are used as source of inelastic events for the purpose of the calculation).

The price one pays, however, is quite severe - many hours of painful scanning. Much progress has been done towards reducing this time by placing sophisticated detector equipment downstream of the emulsion target which then allows us to reduce considerably the volume that needs to be scanned. This plan of attack, however, is clearly limited in its potential scope either to beams where the heavy flavor production constitutes a high fraction of the total cross section (e.g. neutrinos where the technique has proven to be very successful) or to experiments where the downstream detector can preferentially pick out charm events either at the trigger stage (very hard) or in off-line analysis. Otherwise the scanning effort again becomes quite prohibitive. Clearly at the root of all of these difficulties lies

come from another mechanism. Hard gluon emission by higher mass  $c\bar{c}$  pair is postulated as one possible process that could account for these data.

#### PROSPECTS FOR THE FUTURE

There are several second generation experiments either in the planning stage or already taking data that will elucidate some of the questions posed above. However I feel that the main impact in the future on "naked" charm experiments will come from the technological development that is at present going on in the field of good spatial resolution detectors. The lifetimes of charm ground states are now established to lie between  $10^{-13}$  and  $10^{-12}$  secs; the estimates for the bottom states lie between  $10^{-14}$  and  $10^{-13}$  secs. Thus capability of "seeing" tracks in the range of 100-1000 microns would allow one to identify unambiguously presence of short lived particles. I would like to end this review with a few words about the present status of some of these detectors.

a) emulsions. This is the classical detector for looking at events with the ultimate spatial resolution.

the intrinsic very poor time resolution of the emulsion and the great deal of time necessary to scan even a small volume of the emulsion. The relatively small target size due to high cost of emulsion and its processing is also a serious limitation on the use of this technique in the neutrino experiments.

b) high resolution streamer chamber. The pioneering work on this kind of a detector and the first physics results have already been published<sup>10)</sup> by the Yale group. This is clearly not an easy technique but many complex technical problems have been already overcome and one can see a way to improve considerably the state of the art here.<sup>82)</sup> Clearly, the big advantage one has here over emulsions is the much better time resolution of the streamer chamber and intrinsically much easier scanning job, one that probably could be adopted to full automation.

c) high resolution bubble chamber. This appears to be one of the most promising developments in the field. The viability of the technique has been demonstrated by the LEBE NA13 experiment<sup>7)</sup> that observed several examples of charm associated production in  $\pi^-p$  interactions. The identification of charm was done entirely by detecting short lived decays. The value of the cross section obtained ( $\sim 40 \mu\text{b}$ ) is dependent on the lifetimes of the produced particles but appears to agree quite well with other experiments (Fig. 35 and Table I). This technique is being applied at present in a much more fully instrumented NA16 experiment that studies 360 GeV pp and  $\pi p$  interactions.

Another very promising prospect, described at this conference by Montanet,<sup>83)</sup> is the possibility of using holography to increase the depth of the field of view. The early results with a test setup

look quite impressive and give bubble sizes as small as 8 microns.

d) solid state detectors.

Development of high resolution solid state detectors would allow one to dispense with the scanning phase of the experiment, which appears crucial to the other 3 techniques discussed above. A silicon active target, composed of 40 300  $\mu\text{m}$  wafers, has been used by the FRAMM collaboration<sup>54)</sup> to study the diffractive charm photoproduction at the SPS.

The technique relies on a sudden increase in pulseheight (Fig. 36) as one goes from one wafer to the next, corresponding to a multibody decay of a D meson. The potential candidate events are then fully analyzed by using the

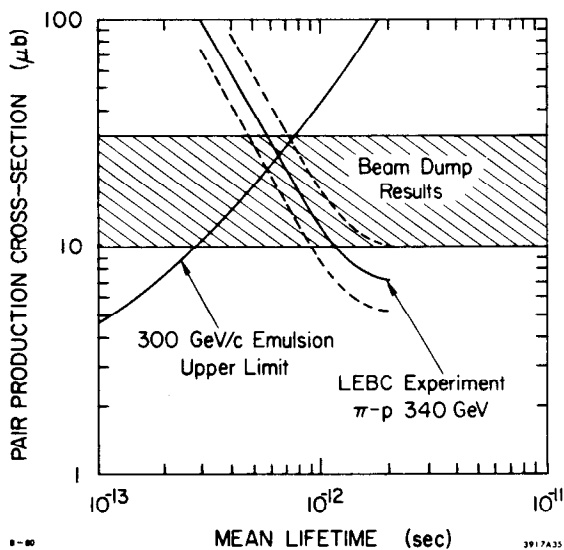


Fig. 35. Results of charm production cross section from the LEBE experiment and comparison with other results.



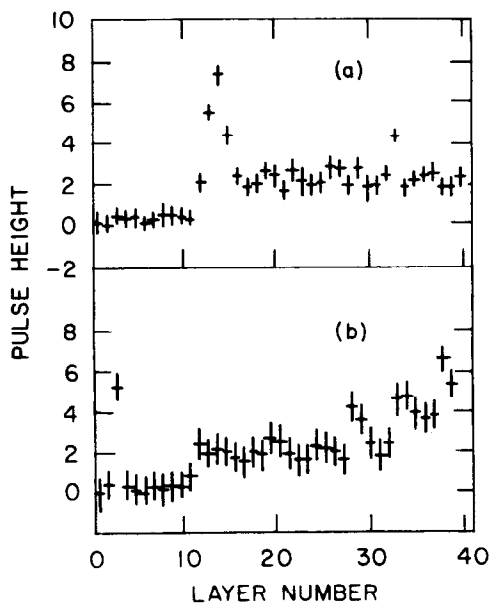


Fig. 36. 2 examples of pulse-height distribution from the active target in the FRAMM experiment: a) inelastic event, b) candidate for  $D^0\bar{D}^0$ , with the production occurring near wafer 3 and the 2 decays near wafer 11 and 34.

information from the downstream spectrometer, Čerenkov counters, and photon detectors. The preliminary analysis shows already evidence of a diffractive mass peak around 4 GeV which appears to decay into D's and/or D\*'s.

The technique as used in this experiment is clearly specialized to diffractive photoproduction. On the other hand work is in progress on expanding the method by also reading out the transverse dimension which would increase the versatility of the detector. It should finally be noted that the 3 visual methods discussed above rely essentially on detecting the transverse displacement of the decay track from the production vertex and thus their efficiency is relatively beam energy independent. The FRAMM detector, however, actually "measures" the length of the decay track and thus its efficiency increases with the beam energy.

#### ACKNOWLEDGEMENTS

I would like to thank my scientific secretaries: G. Fanourakis, T. Y. Ling and F. Messing for their help during the conference, and all the speakers in the relevant sessions for taking the time to explain their results to me.

#### DISCUSSION

Q1: Conversi, Rome: I wish to make two short remarks. One refers to the mass of the  $\Lambda_C^+$  baryon. The first example of neutrino induced production and decay of a  $\Lambda_C^+$  was obtained in CERN experiment WA17 and published last year in Physical Review Letters together with the first estimate of the charmed particle lifetime. The mass of the  $\Lambda_C^+$  reported there (and also at the Bergen and Geneva EPS Conferences) has been readjusted through a further analysis and it will appear in the final paper of that experiment, now in press in "Nuclear Physics." Also, this new mass value (only slightly smaller than that previously reported) agrees, within the error, with the average value of  $M(\Lambda_C^+)$  reported in your talk.

As a second comment, I feel it is worth mentioning here that a search for associated production of beauty particles is being carried out now by an enlarged collaboration, after an exposure made at CERN

just before the SPS shutdown. This is CERN experiment NA19 (spokesman P. Musset), which uses again a hybrid technique and aims at observing the decay sequence: beauty-charmed-ordinary hadrons, in the emulsion.

Q2: Prentice, Toronto: The comparison of charm photo production with photon total cross section measurements needs some clarification. The rise with energy of the hadronic photon total cross section is related to the rise of all the other hadronic total cross sections in the same energy range and is about equally well understood. The rise can be estimated from the behavior of the  $\rho$ ,  $w$ ,  $\phi$  diffractive photoproduction. The  $\phi$  cross section rises almost 40%. The charm cross section can be estimated by the excess of the photon total cross section over the estimate of the contribution from light quark vector mesons. This excess is about 2  $\mu\text{b}$  which is not far from what is seen in the photoproduction reactions.

Q3: Lipkin, Weizmann/Fermilab/Argonne: The charmed baryons produced in hadronic interactions might be polarized (like hyperons) and give an asymmetry in the decays relative to the production plane. A simple check with low statistics would be to separate events with the decay baryon emitted in the upper and lower hemispheres relative to the production plane, i.e., according to the sign of  $\vec{p}_i \times \vec{p}_{\Lambda_c} \cdot \vec{p}_d$ , where  $\vec{p}_i$ ,  $\vec{p}_{\Lambda_c}$  and  $\vec{p}_d$  denote the momenta of the incident beam, the charmed baryon and the decay baryon respectively. The difference between the two distributions would have automatic background subtraction. A signal would indicate a parity violation. If this effect exists, it would be both interesting and useful in analyses.

Q4: Jones, Michigan: The dramatic rise in  $\sigma_c$  reported from the ISR (if confirmed) plus the A dependence of charm production suggests an engineering remark which may not have occurred to everyone; as we go to much higher energies (Tevatron and Pentavac) it is probable that the traditional means of generating  $\mu$  and  $\nu$  beams from  $\pi$  and K decay will give way to beam dump sources.

Q5: Devlin, Rutgers/Fermilab: I would like to add to your list of detection techniques a new device developed by Douglas Potter of Rutgers. It is a triggerable detector/target which has been operated in two modes. First, as a scintillation camera and, second, with a micro-channel plate. The parameters are available in preprint which was submitted to this conference.

Q6: Isgur, University of Toronto: Is the ISR  $\Lambda_c^+$  signal consistent with the observed 50 - 100 MeV width of the  $\Sigma(2250)$ ?

A6: Wojcicki: Maybe the people from ISR would like to comment. The width is very narrow and consistent with resolution. However the peak is removed from the value of 2.285 by the amount comparable to the resolution, or maybe more than the resolution. I'm told by the SFM people that such a shift is not inconsistent with their present understanding of systematics. On the other hand Lanmshade magnet people believe that their peak could not be displaced by more than 10 MeV from the true value. To make an intelligent experimental comment about this question of width and central value, I think one really has to look at things like the  $K^0$  or  $\Lambda$  peak in the same

apparatus, in the same region, and try to extrapolate from that. But that has not really been done for a variety of reasons, and therefore the answer to these questions is still up in the air. It seems to me that some statistical fluctuation may be going on here; it is certainly not enough to generate a whole effect, but conceivably enough to confuse the questions of central values and the widths.

## REFERENCES

1. Alchi, Fermilab, Kobe, Seoul, McGill, Nagoya, Ohio State, Okayama, Osaka, Ottawa, Tokyo, Toronto, Yokohama Collaboration; paper presented by K. Niu in session B6 at this conference.
2. NA3 collaboration (Saclay, CERN, College de France, Ecole Polytechnique, Orsay) quote  $0.935 \pm 0.025$  for the exponent of A from the study of  $J/\psi$  production at 150 GeV.
3. See for example B. L. Cambridge, Nucl. Phys. B151, 429 (1979).
4. Bologna, Glasgow, Rutherford, Saclay, Torino Collaboration, paper #39 submitted to this conference.
5. Princeton, Saclay, Torino, BNL Collaboration, paper #477 submitted to this conference.
6. Brussels, Helsinki, Liverpool, Mons, Stockholm Collaboration, paper #516 submitted to this conference.
7. NA13 collaboration (Brussels, CERN, Oxford, Padova, Rome, Rutherford, Trieste), paper presented by C. Fisher at this conference; see also CERN/EP/80-49.
8. Tata Institute, paper presented by T. K. Malhotra in session B6 at this conference.
9. A. Chilingarov et al., Phys. Lett. 83B, 136 (1979).
10. J. Sandweiss et al., Phys. Rev. Lett. 44, 1104 (1980).
11. H. Fuchi et al., Phys. Lett. 85B, 135 (1979).
12. K. W. Brown et al., Phys. Rev. Lett. 43, 410 (1979).
13. A. Diamant-Berger et al., Phys. Rev. Lett. 43, 1774 (1979).
14. J. Ritchie et al., Phys. Rev. Lett. 44, 230 (1980).
15. A. E. Asratyan et al., Phys. Lett. 79B, 497 (1978).
16. B. P. Roe, University of Michigan report UMHE 79-2.
17. P. Alibrant et al., Phys. Lett. 74B, 134 (1978).
18. H. Wachsmuth, Proc. of the Lepton-Photon Symposium, Fermilab (1979).
19. CHARM collaboration, paper presented in session A10 at this conference by F. Niebergall.
20. Annecy, CERN, College de France, Dortmund, Heidelberg, Warsaw Collaboration, paper presented in session A9 at this conference by G. Sajot; see also D. Drijard et al., Phys. Lett. 85B, 452 (1979).
21. Reference 20 and D. Drijard et al., Phys. Lett. 81B, 250 (1979).
22. K. L. Giboni et al., Phys. Lett. 85B, 437 (1979): see also papers #346 & 512 contributed by this group to this conference, summarized by F. Muller in session A9.
23. W. Lockman et al., Phys. Lett. 85B, 443 (1979).
24. CDHS collaboration, paper presented by K. Kleinknecht in session A10 of this conference.
25. BEBC collaboration, paper presented in session A10 of this conference.
26. Paper presented by K. W. B. Merritt in session A10 of this conference; see also K. W. B. Merritt, Ph.D. thesis, California Institute of Technology.
27. Illinois, Fermilab, Harvard, Oxford, Tufts Collaboration; paper #618 presented by L. J. Koester in session A9 of this conference.

28. These 3 experiments have been summarized in a paper presented in session A10 of this conference.
29. A. Soukas et al., Phys. Rev. Lett. 44, 564 (1980).
30. P. Coteus et al., Phys. Rev. Lett. 42, 1438 (1979).
31. G. S. Abrams et al., Phys. Rev. Lett. 44, 10 (1980).
32. Daryl DiBitonto, Ph.D. thesis, Harvard University, October 1979.
33. S. J. Brodsky, P. Hoyer, C. Peterson and N. Sakai, NORDITA preprint, submitted to Phys. Lett.
34. Columbia, Illinois, Fermilab collaboration, paper presented by I. Gaines in session A11 at this conference.
35. IIT, Maryland, Stony Brook, Tohoku, Tufts Collaboration, paper #701 presented by T. Kitagaki in session A9 at this conference.
36. Padua, Bonn, CERN, Munich, Oxford Collaboration, paper presented by P. Bossetti in session A9 at this conference.
37. Bari, Birmingham, Brussels, CERN, Ecole Polytechnique, Rutherford, Saclay, London Collaboration, paper #819 presented to this conference; also available as Rutherford report RL-80-019.
38. The LSM collaboration feels that their mass calibration is correct to 10 MeV (private communication from F. Muller). The SFM group is much less certain of their absolute mass calibration because of the great complexity of the MWPC system and the difficulty of making sure that all components of the system are correctly aligned. Thus they do not exclude possibility of a 25 MeV shift (D. Drijard-private communication).
39. W. Bacino et al., Phys. Rev. Lett. 45, 228 (1980).
40. M. Barone et al., Nucl. Phys. B132, 29 (1978); L. Baum et al., Phys. Lett 60B, 485 (1976).
41. This group finds the ratio of the observed number of  $\nu_e$  interactions to the expected number to be  $1.2 \pm 0.2$  (BEBC TST group-private communication).
42. J. P. Leveille and T. Weiler, Nucl. Phys. B147, 147 (1979); M. Glück and E. Reya, Phys. Lett. 79B, 453 (1978) and 83B, 98 (1979).
43. Berkeley, Princeton, Fermilab Collaboration, paper presented by A. Clark in session A9 at this conference.
44. European Muon Collaboration (CERN, DESY, Freiburg, Kiel, Lancaster, LAPP, Liverpool, Oxford, Rutherford, Sheffield, Turin, Wuppertal), paper presented by R. Mount in session A9 at this conference.
45. A. R. Clark et al., paper #555 submitted to this conference; also available as LBL-10747; submitted to Phys. Rev. Lett.
46. A. R. Clark et al., paper #553 submitted to this conference; also available as LBL-10879; submitted to Phys. Rev. Lett.
47. D. O. Caldwell et al., Phys. Rev. Lett. 42, 553 (1979).
48. J. J. Aubert et al., paper #740 submitted to this conference; also available as CERN-EP/80-61; submitted to Phys. Lett.
49. A. J. Buras and K. J. F. Gaemers, Nucl. Phys. B132, 249 (1978).
50. J. J. Aubert et al., paper #742 submitted to this conference; also available as CERN-EP/80-62; submitted to Phys. Lett.
51. Reference 34; for earlier published work see M. S. Atiya, Phys. Rev. Lett. 43, 414 (1979).

52. Bonn, CERN, Ecole Polytechnique, Glasgow, Lancaster, Manchester, Orsay LAL, Paris VI, Paris VII, Rutherford, Sheffield Collaboration, paper presented by B. d'Almagne in session A11 at this conference.
53. Reference 1 and paper #265 presented by R. Ammer in session B6 of this conference (Kansas, Fermilab, Serpukhov, ITEP - Moscow, Krakow, Dubna, Gos Fotochem-Moscow, Washington Collaboration).
54. NA-1 (FRAMM) experiment - Frascati, Milano, Pisa, Roma, Torino, Trieste Collaboration; paper presented by E. Bertolucci in session A11 at this conference.
55. Paper #755 submitted to this conference by Photon-emulsion Collaboration (Bologna-CERN-Florence-Genova-Madrid-Moscow-Paris-Santander-Valencia) and Omega-photon Collaboration (Bonn-CERN-Glasgow-Lancaster-Manchester-Paris-Rutherford-Sheffield).
56. D. Sivers, J. Townsend, and G. West, Phys. Rev. D13, 1234 (1976).
57. C. Rubbia (HPWF collaboration), XVII International Conference on High Energy Physics, London 1974, p. IV-118.
58. CDHS Collaboration (CERN, Dortmund, Heidelberg, Saclay); paper presented in session C10 at this conference.
59. A. Benvenuti et al., Phys. Rev. Lett 41, 725 (1978).
60. CFNRR Collaboration (Cal Tech, Fermilab, Northwestern, Rochester, Rockefeller) paper presented by M. Shaevitz in session C9 at this conference.
61. Personal communication at this conference to the author from the ITEP, Fermilab, IHEP, Michigan Collaboration.
62. H. Goldberg, Phys. Rev. Lett. 39, 1598 (1977); also M. Shaevitz, private communication.
63. Paper #649 presented to this conference by LBL, Fermilab, Hawaii, Washington, Wisconsin Collaboration.
64. R. Barate et al., paper #184 presented at the 1979 International Conference on Photon and Lepton Interactions, Batavia, Ill.
65. Paper #975 presented by the WALL Collaboration (Saclay, Imperial College, Southampton, Indiana) to this conference; also talk by J. G. McEwen in session A9 at this conference.
66. H. Fritzsche, Phys. Lett. 86B, 343 (1979).
67. R. N. Coleman et al., Phys. Rev. Lett. 44, 1313 (1980).
68. A. Diamant-Berger et al., Phys. Rev. Lett. 44, 507 (1980).
69. Paper #489 presented to this conference by the Fermilab-Stony Brook Collaboration.
70. H. J. Lipkin, in Prospects for Strong Interaction Physics at Isabelle, BNL 50701 (1977).
71. Paper #535 presented to this conference by the BNL-Illinois-Princeton Collaboration.
72. Paper #554 presented to this conference by the Berkeley-Fermilab-Princeton Collaboration; LBL-11009, submitted for publication.
73. NA3 experiment (Saclay, CERN, College de France, Ecole Polytechnique, Orsay Collaboration); paper presented by P. Delpierre in session A9 at this conference.
74. Paper #546 submitted to this conference by Birmingham, CERN, Ecole Polytechnique Collaboration.
75. Paper presented by the NA3 collaboration at the 1979 European Conference on High Energy Physics in Geneva, Switzerland.

76. Paper #342 submitted by the WA11 Collaboration to this conference; also talk by J. G. McEwen in session A9 at this conference.
77. Papers #807 (calorimeter method) and #982 (spectrometer method) submitted by the WA11 Collaboration to this conference.
78. A. R. Clark et al., Phys. Rev. Lett. 43, 187 (1979).
79. J. J. Aubert et al., Phys. Lett. 89B, 267 (1980).
80. See for example T. Weiler, Phys. Rev. Lett. 44, 304 (1980).
81. Paper #743 presented to this conference by the European Muon Collaboration; CERN-EP/80-84, submitted to Phys. Lett.
82. J. Sandweiss, paper presented at this conference in session D4.
83. L. Montanet, paper presented at this conference in session D4.